Energy Levels of Ho^{166}†

H. T. Motz and E. T. Jurney
Los Alamos Scientific Laboratory, University of California, Los Alamos, New Mexico

AND

O. W. B. Schult,* H. R. Koch, U. Gruber, B. P. Maier, and H. Baader
Physik-Department der Technischen Hochschule München, München, Germany
and
Research Establishment of the Danish Atomic Energy Commission, Risø, Denmark

AND

Gordon L. Struble
The Lawrence Radiation Laboratory, University of California, Berkeley, California

AND

Jean Kern‡ and R. K. Sheline
The Florida State University, Tallahassee, Florida

AND

T. von Egidy, Th. Elze, and E. Bieber§
Physik-Department der Technischen Hochschule München, München, Germany

AND

A. Bäcklin‖
Institute of Physics, Uppsala University, Uppsala, Sweden
(Received 31 October 1966)

The high-energy γ-ray spectrum from thermal-neutron capture in natural holmium has been studied over the energy range of 5000 to 6200 keV. Low-energy gamma radiation of the same reaction has been measured from 30 to 750 keV and conversion electrons from 29 to 500 keV. Data from the reaction $Ho^{165}(d,p)Ho^{166}$ have been analyzed. The combination of the results of these experiments yields an energy of 6243±3 keV for the neutron binding in Ho^{166}. The ground-state rotational band is observed with members up to $I=6-$, and the $I=7-$ level is strongly suggested. A $K=3+$ band built on the 190.9-keV isomer, and a $K=4+$ band are disclosed. The $K=3+[523\uparrow-521\downarrow]$ band members are observed up to $I=6+$ and very probably $I=7+$. The $K=4+[523\uparrow+521\downarrow]$ band contains the 4+ and 5+ levels, and the 6+ is indicated. The $1+[523\uparrow-523\downarrow]$ level is strongly populated in the γ-ray cascade following neutron capture. A rotational band superimposed on this state and containing the 2+, 3+, 4+, 5+, and probably 6+ levels is proposed. The heads of the $5+[523\uparrow+521\uparrow]$ and $2+[523\uparrow-521\uparrow]$ bands are suggested at 264 and 430-keV, respectively. The 7− and 8− members of the $[523\uparrow+633\uparrow]$ band are indicated at 5±2 and 136±2 keV, respectively. The $6+[523\uparrow+512\uparrow]$ state at 294±2 keV probably decays through the 289.12-keV γ transition to the 5-keV level. An additional level with spin 4+ or 5+ has been found at 558.56 keV. A 0−(1−) state at 373.13 keV seems to be very weakly excited during the β decay of Dy^{166}, but fairly strongly populated in the (n,γ) process. The precise energies of low-energy (n,γ) transitions permit a very accurate energy determination of most states observed or indicated. It is found that most bands where more than two members have been seen obey the simple rotational formula very accurately, i.e., they have a small value of B, the "rotation-vibration interaction constant." In fact, the rotation of Ho^{166} is observed to be more perfect than that of neighboring even-even nuclei in the ground-state configuration. The γ-ray transition probabilities for intraband transitions obey the normal Alaga rules, and the constancy of the strength parameter, C^2/q^2, gives additional evidence for band assignments. A calculation of the energies of low-lying levels in Ho^{166} shows good agreement with the observed level energies. The partial cross section for thermal-neutron excitation of the 1200-year state of Ho^{166} has been found to be 3.5±0.5 b by a measurement of the ratio of 1200-year to 27.74-h activities.

I. INTRODUCTION

A STRONG negative pairing energy generally causes the completely saturated even-even nucleus to have a lower total energy than its double unsaturated odd-odd isobaric partners. This results in odd-odd nuclei above O^{16} being unstable. The β-decay selection rules from an 0+ ground state of an even-even parent, still further away from the bottom of the mass valley, demand that only low spin states in the

† Work supported under the U. S., Danish, and Swedish Atomic Energy Commissions and Fonds National Suisse de la Recherche Scientifique.

* Present address: Florida State University, Tallahassee, Florida.

‡ Present address: Université de Fribourg, Fribourg, Switzerland.

§ Present address: Argonne National Laboratory, Argonne, Illinois.

‖ Present address: Forskingsradens Laboratorium, Studsvik, Nyköping, Sweden.

daughter be appreciably populated, thus imposing strong limitations on the possibility of studying excited states of odd-odd nuclei in decay-scheme spectroscopy. Furthermore, the short lifetime of most of the odd-odd nuclei does not permit their levels to be studied through Coulomb excitation. For these reasons, the most satisfactory method for studying odd-odd nuclei is through the use of reaction spectroscopy. The generally high level density of odd-odd nuclei, in particular the heavier ones, requires that such studies be made with the very highest resolution possible.

In the particular case of Ho^{166} the unusually high cross sections involved in the double neutron capture by Dy^{164} has allowed a partial investigation of low-lying states in Ho^{166} through detailed studies[1–5] of the decay of 80-h Dy^{166}. Levels at 54.2 keV (2−) and 82.5 keV (1−) have been assigned as rotational states built on the 0− ground state,[6,7] for which the configuration [523↑−633↑] has been proposed.[8] This assignment is expected for the 67th proton (523↑) and the 99th neutron (633↑) in their lowest Nilsson orbitals.[9] The 0− state of Ho^{166} decays[6] to Er^{166} with a half-life of 27.74±0.05 h.[10]

A state of high spin is also populated in the (n,γ) reaction and also decays[11] to Er^{166}. Its half-life has been measured to be 1200 years[12] and it is believed[8] to be the $K=7-$ state corresponding to the [523↑+633↑] configuration. The Gallagher-Moszkowski rules[13] predict that the 7− state should be the ground state of Ho^{166}. However, Struble and Rasmussen[14] have suggested that relatively larger configuration mixing in the 0− state than in the 7− state lowers the 0− state so that it becomes the ground state in this case. Experimentally, the energy of the 7− state with respect to the 0− level in Ho^{166} is given as −9±33 keV from the work of C. J. Gallagher, Jr., O. B. Nielsen, O. Skilbreid, and A. W. Sunyar (as quoted in Ref. 8), -12_{-11}^{+16} keV by decay scheme studies,[15] and +9±3 keV in (d,p) reaction studies.[16,17] The 0−, 1−, and 2− levels in Ho^{166} are also populated by means of weak γ rays from a state at about 426 keV clearly characterized as having spin-parity 1+. The small logft value for the beta branch feeding this level requires an allowed unhindered β transition strongly suggesting a $K=1+$[523↑−523↓] assignment[8] for the 426-keV state. In contradiction to this, the branching ratio of the γ transitions depopulating the level favors a predominantly $K=0$ assignment.

Helmer and Burson[1] have observed an extremely weak γ ray of about 290 keV in coincidence with the 82.5-keV transition depopulating the 1− state. The 290-keV line has previously not been detected in singles spectra and is believed[1] to originate from a level at 373 keV.

A short-lived isomeric state at 191 keV was inferred from neutron-capture observations of Draper,[18] using a pulsed neutron source, and was confirmed by Alexander.[19] The decay of this isomeric state has recently been investigated in detail by Bjørnholm *et al.*,[20] using in part some of the results of the low-energy neutron-capture work reported in this paper.

Several neutron capture experiments on holmium have been reported in the literature. The early data were obtained with scintillation counters.[21–25] Orecher[26] performed a precise measurement of the strongest low-energy γ transitions using a crystal spectrometer. Motz and Jurney,[27] Groshev and Shadiev,[28] and Groshev and Shadiev[29] measured high-energy (n,γ) lines, and the Riga group observed conversion electron, lines[30] and assigned these to 23 γ-ray transitions. Through these experiments a first step was made toward an extension of the Ho^{166} level scheme beyond that obtained from the Dy^{166} decay scheme work. A more extensive level

[1] R. G. Helmer and S. B. Burson, Phys. Rev. **119**, 788 (1960).
[2] J. S. Geiger, R. L. Graham, and G. T. Ewan, Bull. Am. Phys. Soc. **5**, 255 (1960); in *Proceedings of the International Conference on Nuclear Structure, Kingston, Canada, 1960* (University of Toronto Press, Toronto, Canada), p. 610.
[3] L. I. Rusinov, A. V. Borovikov, V. S. Gvozdev, G. D. Porsev, S. L. Sakharov, and Yu. L. Khazov, Zh. Eksperim. i Teor. Fiz. **39**, 1529 (1960) [English transl.: Soviet Phys.—JETP **12**, 1064 (1960)].
[4] R. Gunnink and A. W. Stoner, Phys. Rev. **126**, 642 (1962).
[5] V. Brabec, O. Bergman, Y. Grunditz, E. Aasa, and S. E. Karlsson, Arkiv Fysik **26**, 511 (1964).
[6] R. L. Graham, J. L. Wolfson, and M. A. Clark, Phys. Rev. **98**, 1173 (1955).
[7] L. S. Goodman, W. J. Childs, R. Marrus, I. P. K. Lindgren, and Y. Cabezas, Bull. Am. Phys. Soc. **5**, 344 (1960).
[8] C. J. Gallagher, Jr., and V. G. Soloviev, Kgl. Danske Videnskab. Selskab, Mat. Fys. Skrifter **2**, No. 2 (1962).
[9] S. G. Nilsson, Kgl. Danske Videnskab. Selskab, Mat. Fys. Medd. **29**, No. 16 (1955).
[10] H. Daniel and G. Th. Kaschl, Nucl. Phys. **76**, 97 (1966).
[11] J. E. Cline and C. W. Reich, Phys. Rev. **129**, 2152 (1963).
[12] K. T. Faler, J. Inorg. Nucl. Chem. **27**, 25 (1965).
[13] G. J. Gallagher and S. A. Moszkowski, Phys. Rev. **111**, 1282 (1958).
[14] G. L. Struble and J. O. Rasmussen, Phys. Letters **17**, 283 (1965).
[15] C. W. Reich (private communication).
[16] G. L. Struble, N. Shelton, and R. K. Sheline, Phys. Rev. Letters **10**, 58 (1963).
[17] G. L. Struble, J. Kern, and R. K. Sheline, Phys. Rev. **137**, B772 (1965).
[18] J. E. Draper, Phys. Rev. **114**, 268 (1959).
[19] K. F. Alexander and V. Bredel, Nucl. Phys. **17**, 153 (1960).
[20] S. Bjørnholm, J. Borggreen, H. J. Frahm, N. J. Sigurd Hansen, and O. Schult, Phys. Rev. **140**, B816 (1965).
[21] V. V. Sklyarevsky, E. P. Stepanov, and B. A. Obinyakov, At. Energ. (USSR) **4**, 22 (1958).
[22] A. S. Melioranskii, I. V. Estulin, and L. F. Kalinkin, Zh. Eksperim. i Teor. Fiz. **40**, 64 (1961) [English transl.: Soviet Phys.—JETP **13**, 43 (1961)].
[23] I. V. Estulin, A. S. Melioranskii, and L. P. Kalinkin, Nucl. Phys. **24**, 118 (1961).
[24] L. F. Kalinkin, A. S. Melioranskii, and I. V. Estulin, Izv. Akad. Nauk. SSSR, Ser. Fiz. **25**, 1124 (1961).
[25] M. Giannini, D. Prosperi, and S. Sciuti, Nuovo Cimento **27**, 538 (1963).
[26] S. Orecher, Z. Naturforsch. **18a**, 576 (1963).
[27] H. T. Motz and E. T. Jurney, Bull. Am. Phys. Soc. **9**, 31 (1964).
[28] L. V. Groshev and N. Shadiev, in *Proceedings of the International Conference on Nuclear Physics, Paris, 1964* (Centre Nacional de la Recherche Scientifique, Paris, 1964), Vol. II, p. 585.
[29] L. V. Groshev and N. Shadiev, Izv. Akad. Nauk. SSSR, Ser. Fiz. **29**, 782 (1965).
[30] M. K. Balodis, V. A. Bondarenko, P. T. Prokofjev, and L. I. Simonova, Nucl. Phys. **66**, 325 (1965).

scheme has been proposed by Struble, Shelton, and Sheline,[16] and Struble, Kern, and Sheline,[17] utilizing the (d,p) reaction and comparing the experimental data with a theoretical model.

In this paper we report the combined approach of five different groups using four different reaction-spectroscopy methods which have developed to the point where it is now possible to attempt a detailed study of the intricate level scheme of Ho^{166}. The methods employed and the laboratories at which the experimental work was done are: (a) high-energy γ-ray spectroscopy, using the reaction $Ho^{165}(n,\gamma)Ho^{166}$ with thermal neutrons, at the Los Alamos Scientific Laboratory; (b) low-energy neutron capture γ-ray spectroscopy using the curved crystal spectrometer at Risø; (c) spectroscopy of conversion electrons from the $Ho^{165}(n,e^-)Ho^{166}$ process using the equipment both at Munich and Studsvik; and (d) proton spectroscopy from the $Ho^{166}(d,p)Ho^{166}$ reaction at Florida State University. Part of the data obtained from the (d,p) reaction process has been published and interpreted previously.[17] Further (d,p) data have been used in this work. The combination of the data obtained in all our experiments permits the construction of three rotational bands and indicates the existence of still other bands. The information about the Ho^{166} level scheme presented in this work provides a basis for the further development and interpretation of the level scheme of Ho^{166}.

The organization of the remainder of this paper is as follows:

II. THEORY

Although our experimental results have been interpreted independently of model consideration as far as possible (see Discussion, Sec. IV) we have found that one can considerably extend this interpretation through the use of models for the nuclear structure of Ho^{166}. In particular, arguments concerning (d,p) reaction cross sections, $M1$ and $E2$ branching ratios, and the existence of anomalous effects in collective rotational structure may be understood on the basis of certain assumptions about the low-energy structure which is contained in a mathematical model. The success of the model is determined by its ability to predict gross qualitative features and to quantitatively reproduce details of the experimental spectrum.

We will describe a model in this section of the paper but in order not to obscure the simple qualitative predictions, the mathematical detail has been relegated to Appendix B. The qualitative success can be judged from the interpretation of experimental data in the subsequent sections. In Sec. V a comparison is made between the quantitative predictions and the experiment.

The success of the model of Bohr and Mottelson,[31] Nilsson,[9] and Kerman,[32] in explaining the spectra of odd-A deformed nuclei suggested that a similar approach might apply to odd-odd nuclei. Basically, then, an attempt was made to understand the levels in Ho^{166} in terms of the coupling of the odd-neutron and odd-proton in the presence of the Dy^{164} core. Plausibility arguments explaining why this should be a good description and how it differs from the problem of two particles in a deformed well are considered in the Appendix. To a good approximation, it is hoped the Hamiltonian may be written as

$$H=H_{\mathrm{R}}+H_{\mathrm{RPC}}+H_{\mathrm{PP}}+H_p+H_n+H_{\mathrm{INT}}. \quad (1)$$

H_{R}, H_p, H_n describe the motion of a proton and neutron in a deformed well which may rotate and H_{RPC} and H_{PP} describe the rotational particle and particle-particle coupling. Assuming that the field generated by the core is such that the states of the last proton and neutron are described separately by Nilsson[9] wave functions, the states of the odd-odd system may be written explicitly as a direct product and form a basis for the diagonalization of the entire model Hamiltonian. Indeed if the other terms are small, it may give a good description of the actual nuclear system. The invariance of the Hamiltonian under certain symmetry operations then requires that $K=|\Omega_p\pm\Omega_n|$ where we are considering a state in which the neutron and proton are in Nilsson orbitals which have values of the projection of the angular momentum along the symmetry axis of Ω_p and Ω_n. K is the projection of the total angular momentum along this

[31] Å. Bohr and B. R. Mottelson, Kgl. Danske Videnskab. Selskab, Mat. Fys. Medd. **27**, No. 16 (1953).

[32] A. K. Kerman, Kgl. Danske Videnskab. Selskab, Mat. Fys. Medd. **30**, No. 15 (1956).

TABLE I. Experimentally asssigned Nilsson states in odd-A isotopes and isotones of Ho^{166}.

Nilsson state	Observed in	Excitation energy (keV)	Single-particle energy[a] (keV)	Ref.	Comments
$\frac{7}{2}-[523\uparrow]$	Ho^{165}	0	−42	33	
$\frac{3}{2}+[411\uparrow]$	Ho^{165}	361	343	33	May be hole excited
$\frac{1}{2}+[411\downarrow]$	Ho^{163}	305	400[b]	34	
$\frac{7}{2}+[633\uparrow]$	Dy^{165}	0	−42	35	
$\frac{1}{2}-[521\downarrow]$	Dy^{165}	108	109	35	
$\frac{5}{2}-[512\uparrow]$	Dy^{165}	184	154	35	
$\frac{5}{2}-[523\downarrow]$	Dy^{165}	535	505	35	Hole excited
$\frac{3}{2}-[521\uparrow]$	Dy^{165}	605	587	35	c

[a] The single-particle energy is obtained from the excitation energy by subtracting zeroth- and first-order rotational contributions. The energies of the zeroth-order states in Ho^{166} are obtained by adding the single-particle proton and neutron energy and zeroth-order rotational contribution.

[b] This state was known only in Ho^{163} at the time these calculations were performed. It was arbitrarily chosen to give a single-particle energy of 400 keV in Ho^{165}. Since that time, this state has been observed in Ho^{165} at 429.4 keV [J. W. Starner and M. E. Bunker, Bull. Am. Phys. Soc. **9**, 18 (1964)].

[c] This state was erroneously assumed to be a particle state in the calculations. A later and better value for the energy is given in Ref. 65. The effect of these assumptions on the results would be minor.

axis. For specific Nilsson orbitals, the two distinct K states will not be degenerate but will be split because the state with larger K will have a higher rotational energy. If H_{RPC}, H_{PP}, and H_{INT} are negligible, the model makes simple predictions for the energy spectrum. One must look at the energy spectra of Ho^{165} and Dy^{165} to find the energy of the Nilsson orbitals for the proton and neutron, remove the rotational contribution to this energy, and find the various proton-neutron combinations. Their predicted energy in Ho^{166} will be the sum of the Nilsson energies plus the rotational energy for the odd-odd system. Thus, in Table I, the several Nilsson states are listed which are found experimentally in Ho^{165} and Dy^{165}.[33–35] Using this table and following the prescription, it can be predicted that there should be at least three low-lying doublets, viz.,

$$[523\uparrow\pm 633\uparrow](K=0-,7-),$$
$$[523\uparrow\pm 521\downarrow](K=3+,4+),$$

and

$$[523\uparrow\pm 512\uparrow](K=1+,6+).$$

It is well known that the remaining terms in the Hamiltonian are not negligible. First consider H_{INT}, the neutron-proton residual interaction, which has a great influence on the spectrum. It will often cause the state in a configuration doublet with higher rotational energy to lie lower in energy and these effects are remarkably well predicted by the Gallagher-Moszkowski[13] coupling rules. The Gallagher-Moszkowski rules predict the relative position of the two K members of a configuration and may be stated succinctly that the lower member of such a doublet is the predominantly triplet state. These rules have recently been theoretically justified by De Pinho and Picard[36] using a force of the form

$$V_{np}=V(|r_{np}|)[1-\alpha+\alpha\boldsymbol{\sigma}_p\cdot\boldsymbol{\sigma}_n]. \quad (2)$$

They found the Gallagher-Moszkowski rules to be preserved in all cases that were examined for positive values of α.

Another effect, the displacement of the even members relative to the odd members in the $K=0$ rotational band, was first quantitatively discussed by Newby.[37] This displacement is explained by the symmetry of the state vector and virtually any nuclear force except a pure Wigner force will contribute. Finally the force is often sufficiently strong to reorder the relative positions of the states that arise from different configurations. This will be discussed quantitatively in Sec. V.

The H_{RPC} and H_{PP} terms involve couplings between the individual-particle angular momentum and the total angular momentum, and the angular momenta of the two particles. These are usually smaller because, with one exception, they arise in second order, and the first-order effect in H_{PP} is again a displacement between the odd and even members of $K=0$ rotational bands. Often their effect on energy systematics can be compensated by renormalization of moments of inertia in the affected rotational bands, but the K mixing in the state vectors has important consequences in calculating spectroscopic factors and reduced transition probabilities.

Collective modes of excitation of the core other than rotation in the Hamiltonian have been neglected. This was done because collective states in odd-odd deformed nuclei have not yet been characterized and because only the low-energy portion of the spectrum where effects should be small compared with errors inherent in the shell-model calculation is considered. This simplifies the numerical work considerably. But with great precision to which the energy levels within several bands are known, the effects of the rotation vibration interaction are observed and can be accounted for in perturbation theory by the familiar $BI^2(I+1)^2$ correction to the rotational energy within a band.

III. EXPERIMENTAL METHODS AND RESULTS

A. The High-Energy Neutron Capture Gamma Spectrum

Ho^{165} is monoisotopic with a thermal-neutron absorption cross section of 64 b,[38] and has a ground-state spin $\frac{7}{2}-$. The capture of slow (s-wave) neutrons thus yields a compound state in Ho^{166} with spin and parity 3− or

[33] R. M. Diamond, B. Elbek, and F. S. Stephens, Nucl. Phys. **43**, 560 (1963).
[34] B. R. Mottelson and S. G. Nilsson, Kgl. Danske Videnskab. Selskab, Mat. Fys. Skrifter **1**, No. 8 (1959).
[35] R. K. Sheline, W. N. Shelton, H. T. Motz, and R. E. Carter, Phys. Rev. **136**, B351 (1964).
[36] A. G. De Pinho and J. Picard, Phys. Rev. Letters **15**, 250 (1965).
[37] N. D. Newby, Jr., Phys. Rev. **125**, 2063 (1962).
[38] H. Pomerance, Phys. Rev. **83**, 641 (1951).

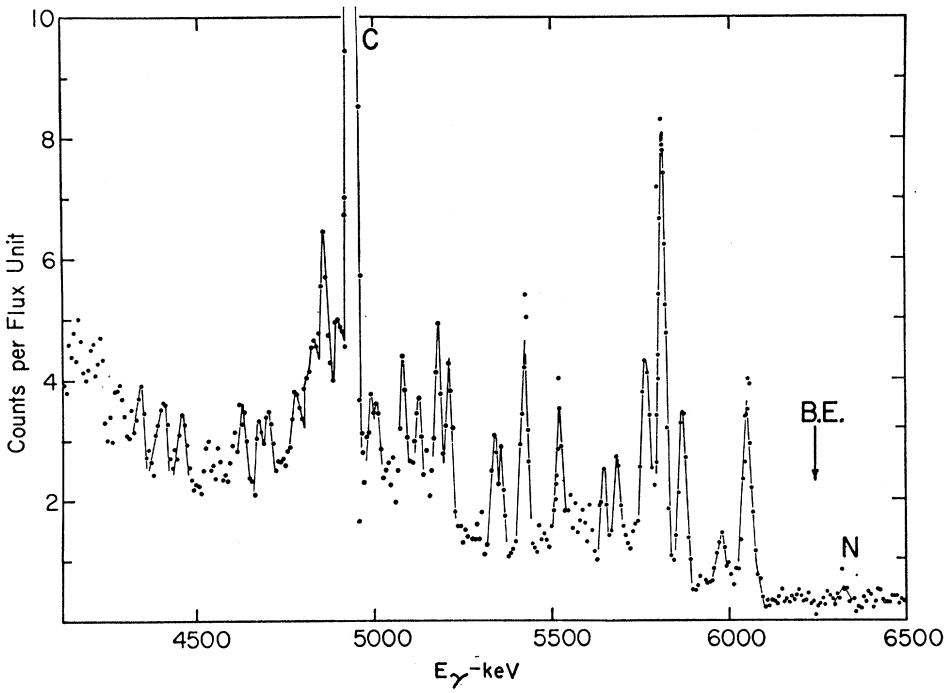

FIG. 1. High-energy (n,γ) spectrum of Ho^{166}, determined with Los Alamos magnetic compton spectrometer. (B.E. ≡binding energy.)

4−. It is known[39] that for thermal-neutron absorption, the population of 3− states is (59.4±3)%, so that the remaining component, (40.6±3)%, must then result in population of compound states with spin 4−. These 4− states will decay via strong $E1$ primary transitions to excite states with spin and parity 3+, 4+, and 5+ and $E1$ primary radiation from the 3− compound states will populate states of 2+, 3+, and 4+ spin-parity. Weak $M1$ primary transitions will populate levels with the same spins, but with opposite parity.

These primary transitions have been measured using both a magnetic Compton spectrometer and a lithium-drifted germanium detector. The Los Alamos magnetic Compton spectrometer[40] was used to observe the spectrum from a 100-g sample of Ho oxide from 4.0 to 6.5 MeV. This instrument consists of a double-focusing magnet having $\rho_0=35$ cm and utilizes four electron detectors and coincidence detection of backscattered quanta in either of two detectors. The nonlinearity is less than 2 keV from 2.5 to 11 MeV. Thus, the dominant error entering into energy differences is the statistical one of determining line energies and need not involve the absolute energy scale error. Two scans (A and B) were made over most of the energy range of 4.0 to 6.5 MeV, but scan B was interrupted and required magnet recycling. Scan A is shown in Fig. 1 and Table II, and provides accurate relative energy measurements for all lines that can be resolved. Since the ground-state transition of $C^{12}(n,\gamma)C^{13}$ is present from the graphite moderator, the $Ho^{165}(n,\gamma)Ho^{166}$ energy calibration can be conveniently confirmed with reference to this carbon line. The measured carbon ground-state line value was 4944.7 keV, in close agreement with the accepted value. This energy was determined from least-squares fitting to within a statistical error of 0.2 keV. The absolute error of the spectrometer in the 5-MeV region is less than 2 keV as determined from the Mg^{24} γ ray of 2753.98±0.3 keV. The absolute error in the 6-MeV region is less than 2.5 keV. A combination of the absolute error of ±2.5 keV with the relative energy errors listed in Table II gives the absolute errors of the Ho lines. Where lines have not been resolved, the energies and errors in Table II refer to the centroid of the actual lines present. For a comparison of the results obtained during this experiment with the data given by Groshev *et al.*,[28] see Ref. 41.

The spectrum in Fig. 2 was obtained using a 3-mm deep Li-drifted Ge detector inside a large NaI scintillation detector operated in coincidence to accentuate the double-escape peaks. This NaI annulus (30 cm long, 20-cm o.d., 6.5-cm inside bore diam) was previously used as an anticoincidence detector with a centrally located scintillation crystal.[40] The target for this facility is inside a bismuth pipe which is also located inside the graphite thermal column of the Omega West Reactor. The target is 6 m away from the detector which views only the target. Background effects are greatly minimized by this geometry. The annulus is not split

[39] R. I. Schermer, Bull. Am. Phys. Soc. 8, 334 (1963); Phys. Rev. 136, B1285 (1964).

[40] H. T. Motz and G. Bäckström, *Alpha, Beta, and Gamma Ray Spectroscopy*, edited by K. Siegbahn (North-Holland Publishing Company, Amsterdam, 1965), Chap. XIII, pp. 769–804.

[41] H. T. Motz and E. T. Jurney, in *Proceedings of the International Conference on Nuclear Structure with Neutrons, Antwerp, 1965* (North-Holland Publishing Company, Amsterdam, 1966).

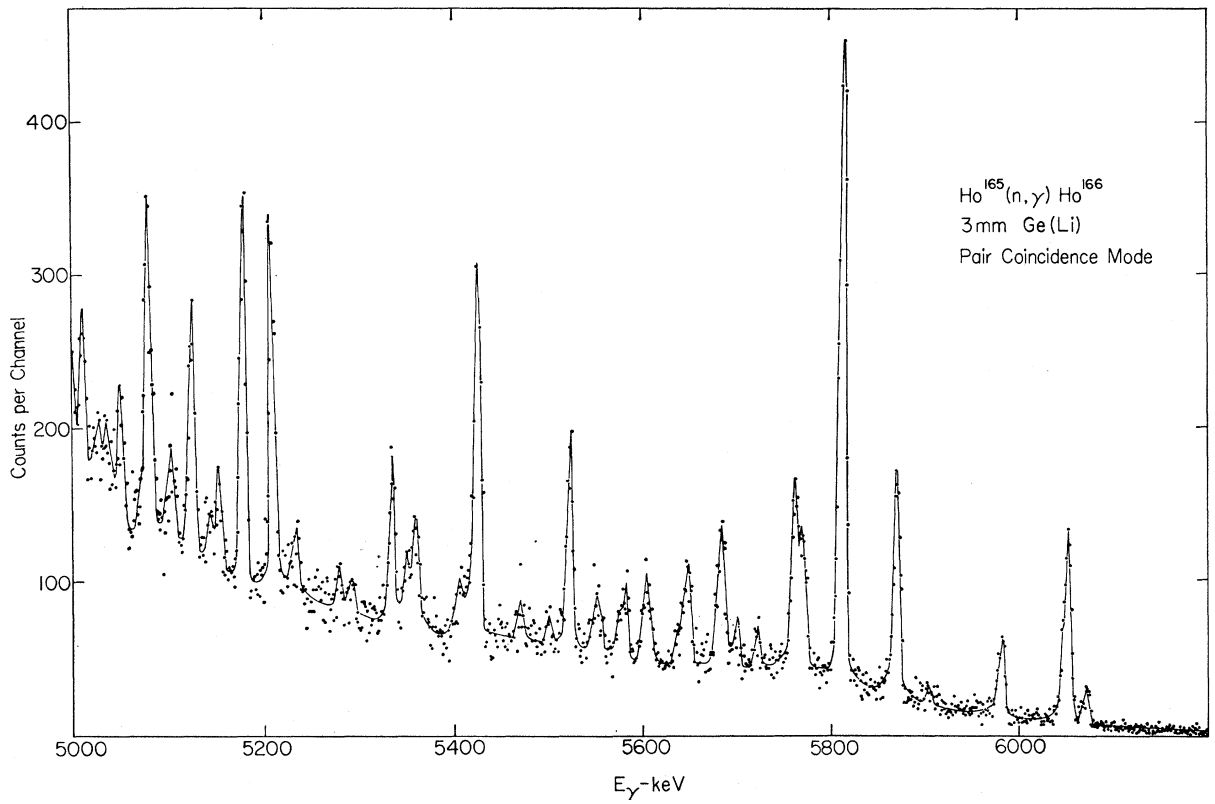

FIG. 2. High-energy neutron-capture γ spectrum of Ho^{166} measured with the Ge(Li) detector at Los Alamos operated as two escape pair spectrometer. The radiation from a 1.5-g holmium target penetrated a 1.0-cm lead absorber. A resolution of 8.0 keV (FWHM) was obtained during the 63.5-h run.

into two sections, so it is not possible to obtain two separate annihilation quanta pulses in coincidence with the Ge pulses. However, a single pulse of 1022 keV $\pm 10\%$ can be used in coincidence. This allows acceptance of some Compton events which contribute to the background. An efficiency of 50% is normally obtained for the double escape Ge peak and an improvement of signal-to-noise of a factor of three was obtained for Ho.

The intensities of the high-energy Ho transitions were determined by comparing the line areas (Ge data) with those in a spectrum of $N^{14}(n,\gamma)N^{15}$, obtained from a weighed target of melamine. Both the capture cross section[41] and the γ-ray branching ratios[42] are known for the nitrogen reaction. The intensities of the transitions in the Compton spectrometer data were normalized to the Ge data with the intense 5812-keV line.

The γ rays from $N^{14}(n,\gamma)N^{15}$ also served as a convenient source for calibrating the energy scale of the Ge data. Although the absolute energies of the N^{15} γ rays are known only to about 1.5 keV, their separation in the 4500–6300-keV region is known to about 0.5 keV.[43] Thus the slope of the Ge energy scale could be determined with good accuracy.

Computer treatment of the data with a least-squares code is done both for the Compton spectrometer data and Ge data. For the Compton spectra, a skewed Gaussian function is used; its width and skewness have been carefully determined for strong single γ rays from various targets from 1–11 MeV. Although the statistical accuracy of the results shown in Table II is very good, it is important to emphasize the limitations of such an analysis which are due to both the constraints imposed and to the resolution. Note that only two lines were fitted in the region of 6052 keV. Since the resolution of the instrument is 23 keV in this energy region, it would be quite unreasonable to fit a third line in this region. This doublet is almost completely resolved with the improved resolution of the Ge detector. The Ge two-escape peaks are fitted with the same code but using a normal Gaussian plus an exponential tail function. Each peak has five parameters, any of which can be fitted or fixed as desired. When the width of a peak is greater

[42] E. T. Jurney and H. T. Motz, in *Proceedings of the International Conference on Nuclear Physics with Reactor Neutrons*, edited by F. E. Throw (Argonne National Laboratory, Argonne, Illinois, 1963), Report No. ANL 6797, p. 236; H. T. Motz, R. E. Carter, and W. D. Barfield, in *Pile Neutron Research in Physics* (International Atomic Energy Agency, Vienna, 1962), p. 225.

[43] R. E. Carter and H. T. Motz, in *Proceedings of the International Conference on Nuclear Physics with Reactor Neutrons*, edited by F. E. Throw (Argonne National Laboratory, Argonne, Illinois, 1963), Report No. ANL 6797, p. 179.

TABLE II. Energies and intensities of high-energy γ transitions from the $Ho^{165}(n,\gamma)Ho^{166}$ reaction.

Compton spectrometer			Ge pair spectrometer				Excited levels	
E_γ (keV)	dE_γ [a] (keV)	I_γ ($\gamma/10^3$ n)	E_γ (keV)	dE_γ [b] (keV)	I_γ ($\gamma/10^3$ n)	dI_γ	E_{ex} [c] (keV)	dE_{ex} (keV)
6073.9	2.5	0.6	6071.0	0.8	0.51	0.1	170.8	0.8
6052.0	0.7	3.5	6051.6	0.7	2.5	0.4	190.9[c]	···
			6044.6	1.5	0.41	0.1	197.9	2
5978.7	1	1.2	5981.3	1	1.1	0.2	263.2	1
(5926	5[d]	0.3						
			5911.8	3	0.1	0.05	330.7	3
			5903.7	2.5	0.15	0.1	338.8	2.5
5870.3	0.5	3.1	5870.1	1.7	3.0	0.5	372.5	0.5
5813.2	0.8	7.6	5812.0	0.6	7.6	1.2	430.1	0.5
5773.1	3	2.1	5770.1	0.8	1.5	0.3	471.8	0.8
5761.2	2	2.3	5761.0	0.7	2.1	0.4	481.6	0.7
			5720.4	1.5	0.33	0.07	522.1	2
(5706	7[d]	0.3						
			5697.8	1.5	0.38	0.07	544.7	1.5
5685.4	2	1.8	5682.9	1	1.8	0.4	558.9	1
5647.7	1	1.3	5648.3	1	1.1	0.2	594.7	0.8
			5640.2	2	0.42	0.1	602.3	2
5606.7	3	0.7	5604.7	1.2	1.0	0.2	637.3	1.2
5581.7	3	0.9	5582.8	1.5	0.63	0.1	659.7	1.5
			5575.9	2	0.39	0.1	666.6	2
			5555.9	2	0.32	0.1	686.6	2
5553	2	0.9	5548.8	1.5	0.54	0.1	693.7	1.5
5524.6	1	2.3	5522.7	1	2.1	0.3	719.1	0.7
			5500.7	2.5	0.18	0.07	741.8	2.5
5470.7	3	0.6	5477.6	2	0.32	0.1	767.8	4
			5458.8	3	0.14	0.1	783.7	3
5426.6	0.6	3.8	5426.4	0.6	3.7	0.6	816.2	0.5
			5412.7	1	0.72	0.2	829.8	1
5360.3	2	1.3	5361.4	1	1.1	0.2	881.6	1
			5351.9	1	0.72	0.2	890.6	1
5339.6	2	1.4	5336.4	1	1.4	0.3	905.2	1
(5289	3[d]	0.6	5281.3	2.5	0.32	0.1	961.6	3
5240	4	0.6	5235.3	1.5	0.42	0.1	1006.0	1.5
5213.3	0.8	3.2	5211.2	1	3.2	0.5	1030.3	0.7
5181.3	0.7	3.4	5179.7	1	3.3	0.5	1062.1	0.7
			5153.2	1.5	0.56	0.2	1089.3	1.5
5144	3	1.6	5143.0	2	0.35	0.1	1099.3	2
5121.9	2	2.0	5126.2	1	2.0	0.4	1117.9	2
			5105.5	1.5	0.71	0.2	1137.0	1.5
5084.0	1	2.9	5080.7	1	2.9	0.5	1160.4	1.5
			5050.8	1	0.75	0.2	1191.7	1
5042	2	1.2	5036.5	2	0.40	0.1	1204	2
			5026.5	2	0.39	0.1	1216	2
5011	2	1.9	5011.1	1	1.2	0.3	1231.6	0.8
4988	2	1.6					1255	2
4944.7	0.2	e						

[a] Statistical error only.
[b] See text.
[c] E_γ=6052.0 (Compton) or 6051.6 (Ge) keV assumed to populate the 190.9-keV level. Other excitations derived relative to this state.
[d] Probable impurity.
[e] $C^{12}(n,\gamma)C^{13}$ ground-state transition.

than the expected value, a doublet is attempted with fixed widths, the values chosen being equal to that obtained for other lines in the spectrum. When the fit for such doublets converges, energy and area errors are larger than for single, isolated lines and errors are anticorrelated. A good example of this is the doublet at (5762,5772) keV which has a separation of 9.8±1.0 keV.

The Q value of the reaction $Ho^{165}(n,\gamma)Ho^{166}$ cannot be obtained from the literature with sufficient accuracy to permit the calculation of the energy of the Ho^{166} levels which are excited through high-energy γ transitions. The best value can be obtained from the Q value of the $Ho^{165}(d,p)Ho^{166}$ reaction published recently by Struble *et al.*[17]: Q=4025±7 keV. Adding to this value the deuteron binding energy, we obtain $Q_{n\gamma}$=6250±7 keV. The intense 6052±0.7-keV γ transition would thus excite a level at 198±8 keV. This value agrees within the experimental uncertainty with the energy 190.90 ±0.006 keV of the Ho^{166} isomer the spin of which is believed to be 3+. The best value for the Q value of the $Ho^{165}(n,\gamma)$ reaction is thus 6243±3 keV (6052+191). Using the 190.9-keV state as a reference level, it is possible to ignore the absolute error in the γ-energy measurement between 5 and 6 MeV. We therefore include in Table VIII only relative errors: those arising from the nonlinearity of the energy scale and the statistical error.

B. The (d,p) Spectrum

Thin holmium targets (both as metal and as oxide) on thin carbon backings ($\sim$20 μg/cm^2) have been bombarded with 11–12-MeV deuterons with the Florida State University Tandem Van de Graaff.[44] The proton spectra have been measured at 25°, 35°, 45°, 60°, 65°, 90°, and 95° with respect to the incident deuteron beam, using a Browne-Buechner magnetic spectrograph.[45,46] The proton groups photographically recorded as a function of plate distance on nuclear emulsion plates have been fitted using a skewed Gaussian to obtain greater accuracy for both energies and intensities.

The results of runs at 45°, 65°, 90°, and 95° have been published previously.[17] The proton groups coming from Ho^{166} nuclei in their lowest excited states are very weak (see Ref. 17, Fig. 1, peaks numbered 0 and 1). A decomposition of these weak peaks which contain only a few proton tracks per $\frac{1}{2}$-mm strip is possible; however, the statistics do not permit a unique decomposition in those cases where the distance of components is only about half of the full width at half-maximum (FWHM) of the proton peaks. For this reason we have assumed in the present work that a very weak proton line corresponds to the excitation of a single level in Ho^{166}. Assuming further that the first strong proton group (the line numbered 7 in Fig. 1, Ref. 17) populates the 190.9-keV level in Ho^{166}, we have fitted[47] the 25°, 35°, and 60° runs and re-evaluated the 45°, 65°, 90°, and 95° runs up to an excitation energy of 400 keV. Our results are for the most part in agreement with the experimental results obtained previously.[17] However, we find no evidence for two proton groups exciting levels at 0±3 and 9±3 keV. Instead, we obtain a level at 5±2 keV on the basis of assumptions mentioned above. All (d,p) runs reveal a proton group corresponding to a Ho^{166} level at an average energy of 136±2 keV. A proton line corresponding to an excitation of a 151-keV level has not been found in the 25°, 35°, and 60° runs. The re-evaluation of the 65° run gave no evidence for this level which previously[17] was believed to be very weakly excited. The intensity of the proton group corresponding to a 151-keV level excited during the 90° run is zero within the statistical error. For these reasons, we think that the 151-keV level clearly seen only in the 45° run is due to an impurity.[17] The energies of the Ho^{166} states populated during the (d,p) reaction are given in Table VIII for comparison with the data derived from the other experiments described in this paper. They have been taken directly from the paper by Struble *et al.*[17] except for the 5- and 136-keV states. The (d,p) and high-energy (n,γ) data are compared in Fig. 3.

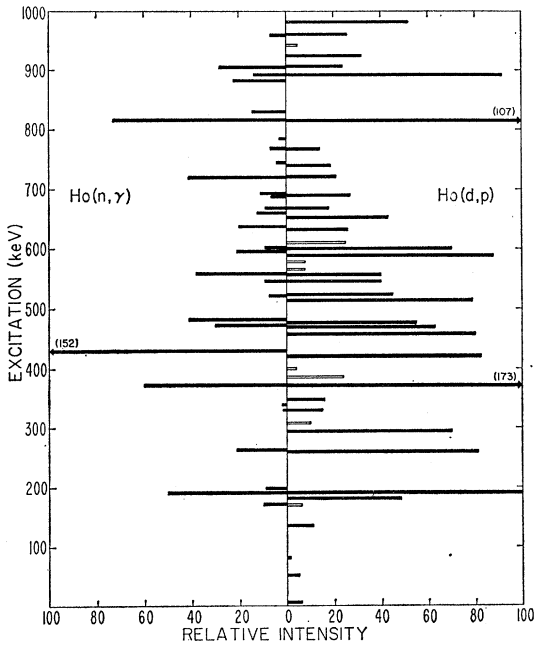

FIG. 3. Bar plot of high-energy (n,γ) and (d,p) lines feeding Ho^{166} states. The lengths of the bars are proportional to the intensity of the corresponding (n,γ) lines or proton groups.

C. The Low-Energy (n,γ) Spectrum

The low-energy neutron-capture γ-ray spectrum has been measured with the curved crystal spectrometer at Risø.[48] The source (60 mg, 99.8% pure Ho_2O_3) was located in the center of one of the tangential through holes of the Danish Pluto-type reactor (DR-3) where the thermal neutron flux is 6×10^{13}/cm^2 sec. Details of the experimental procedure have been described previously.[49] The reflex width was approximately 11 sec of arc, corresponding to a resolution of

$$\Delta E/E = 2\times10^{-5}E/n \quad (E \text{ in keV}), \qquad (3)$$

where n is the order of reflection.

Weak reflexes have been measured in second order. The energies of intense transitions were determined from the third order of reflection and those of very strong lines were obtained from the fifth-order reflexes. Only a few low-energy transitions ($E<60$ keV) were studied in the first-order reflection.

About 350 neutron-capture γ lines were found in the energy region from 27 keV to 1 MeV. A small part of the spectrum is illustrated in Fig. 4(a). The relative energy values E_γ, the uncertainty in relative energy determination dE_γ, resulting only from the measure-

[44] Supported in part by the U. S. Air Force and the Nuclear Program of the State of Florida.

[45] C. P. Browne and W. W. Buechner, Rev. Sci. Instr. **27**, 899 (1956).

[46] R. N. Kenefick and W. N. Shelton, theses submitted to the Graduate School of the Florida State University in partial fulfillment of the requirements of the Ph.D. degree, 1962 (unpublished).

[47] We are very much indebted to H. Kaufman, who kindly made his fitting program available to us.

[48] O. W. B. Schult, B. P. Maier, U. Gruber, and H. R. Koch, Argonne National Laboratory Report No. ANL 6797, 1963, p. 111 (unpublished).

[49] O. W. B. Schult, U. Gruber, B. P. Maier, and F. W. Stanek, Z. Physik **180**, 298 (1964).

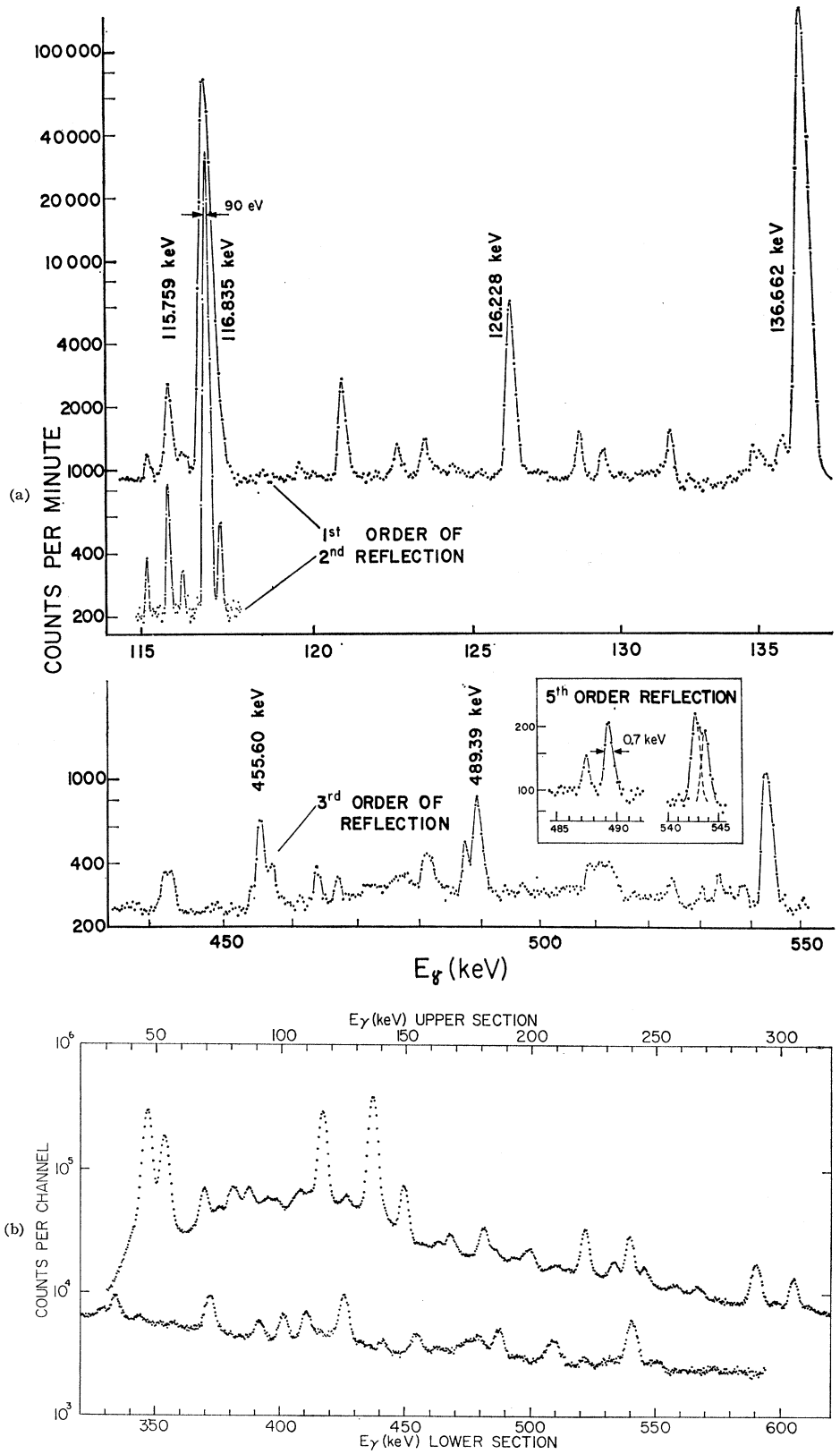

FIG. 4. (a) Small sections of the low-energy (n,γ) spectrum obtained with the diffraction spectrometer. Each point of the first-order reflection spectrum was obtained during a counting period of 80 sec. The corresponding periods were 45 sec for the second-, 10 min for the third-, and 160 sec for the fifth-order spectra. The line at 120.8 keV has not been assigned as transition in Ho^{166} because its intensity increases during the irradiation of the target with slow neutrons. The upper part of the figure shows the improvement of the resolution when going from the first- to the second-order reflection. The actual measurements are usually performed in the third- or fifth-order reflections. The insert in the lower part of the figure clearly shows that the group at 543 keV is complex. The decomposition into a doublet is indicated. (b) Low-energy (n,γ) spectrum of Ho^{166} measured with the Los Alamos Ge(Li) detector inside a NaI annulus in anticoincidence.

TABLE III. Low-energy γ-ray and electron data from $Ho^{165}(n,\gamma)Ho^{166}$. Column I labeled E_γ is the relative γ-ray energy determined with the diffraction spectrometer at Risø. The values given are very nearly equal to the energy in keV; column II labeled dE_γ is the relative error in the energy excluding errors in the conversion of wavelength to energy; column III indicates that the γ ray has been used in the decay scheme if a $\surd$ appears, that more than one γ ray is present if "*c*" (complex) is used. Questionable γ rays are indicated by the symbol "?". Column IV labeled I_γ gives the absolute intensity in γ rays per 100 neutrons captured as measured with the Risø diffraction spectrometer; column V labeled dI_γ gives the relative error in percent of the Risø intensity values in column IV; column VI labeled E gives the approximate γ-ray energy as determined from the Ge(Li) spectrometer at Los Alamos. This value represents only a centroid; the components of the fitted data can be judged from the detailed entries given in columns I and IV and the data shown in Fig. 4(b); column VII labeled I gives the intensities as measured by the Ge(Li) spectrometers. The italicized values are from the Studsvik measurements. Note that integration over many components occurs in most cases as does the energy value in column VI; column VIII labeled dI gives the percentage error of the intensity I; column IX labeled shell refers to the atomic shell(s) in which internal conversion occurs; column X labeled E_e gives the conversion electron energy in keV; column XI labeled I_e gives the relative internal conversion electron intensity; column XII labeled dI_e gives the percentage error in the relative intensity I_e column XI; column XIII labeled α_{exp} gives the measured conversion coefficient. For calibration details see text, Sec. IIIE. The italicized entries for columns X through XIII refer to Studsvik measurements; column XIV labeled $\alpha(E1)$, $\alpha(E2)$, and $\alpha(M1)$ are the theoretical conversion coefficients of Rose; column XV labeled multipolarity, summarizes the electron conversion coefficient data. The following conventions have been used: When an admixture is estimated to be less than 30%, the actual estimated percentage limit is given; when the upper limit of the admixture is greater than 30%, a notation such as $M1(+E2)$ is used; when the measured value falls near the average for two multipoles, a notation such as $M1$, $E2$ or $E2$, $M1$ is used, with the preferred multipolarity listed first.

I E_γ	II dE_γ	III	IV I_γ	V dI_γ	VI E	VII I	VIII dI	IX Shell	X E_e keV	XI I_e	XII dI_e	XIII α_{exp}	XIV $\alpha(E1)$	XIV $\alpha(E2)$	XIV $\alpha(M1)$	XV Multipolarity
38.493	0.006	$\surd$	0.3	30				L_1	29.10	1.4	50	5.2	0.25	0.94	4.1	$M1+(E2)$
46.232	0.004	?	0.02	···												
48.0315	0.0007	$\surd$	0.17	20												
48.303	0.004	?	0.03	···												
51.8155	0.0007	$\surd$	0.23	15												
53.3434	0.0007		0.09	15												
54.2392	0.0007	$\surd$	2.5	10				L_2	45.32	28	30	12.5	0.045	10.9	0.128	$E2+<20\%\ M1$
								L_3	46.17	31	30	13.8	0.060	12.6	0.024	
								M	52.11	12	30	5.4				
								N	53.80	3.6	30	1.6				
57.19	0.010	*c*	0.16	···												
57.469	0.010		0.07	···												
57.517	0.008	$\surd$	0.32	20												
57.83	0.02	?	0.02	···												
66.103	0.007	$\surd$	0.20	20												
69.7604	0.0014	$\surd$	2.8	10				L_1	60.37	1.2 *2.3*	40 *15*	0.48 *0.82*	0.063	0.21	0.78	$M1+<30\%\ E2$
70.988	0.010		0.18	20												
72.8859	0.0015	$\surd$	0.20	20				L_2	63.97	0.5	60	2.8	0.017	2.7	0.054	$E2+<25\%\ M1$
								L_3	64.81	0.8	50	4.5	0.022	2.9	0.010	
74.261	0.016		0.09	30												
75.753	0.016		0.07	30												
75.985	0.008		0.07	30												
76.4663	0.0014	$\surd$	0.34	10	75.7	0.40	···									
76.7258	0.0014		0.19	15												
78.871	0.012		0.05	···												
82.470	0.002	$\surd$	0.97	10	82.7	0.90	25	K	26.86	2.4	50	2.8	0.44	1.60	4.0	$M1(+E2)$
								L_1	73.07	0.4	60	0.46	0.042	0.15	0.48	
83.049	0.014		0.05	30												
84.468	0.010	$\surd$	0.13	25												
84.742	0.014		0.04	30												
86.359	0.011		0.10	25												
86.765	0.011		0.10	25												
87.193	0.015		0.04	30												
87.5946	0.0016	$\surd$	1.24	10	87.0	1.2	···	K	31.98	3.4	30	3.0	0.37	1.41	3.3	$M1+<30\%\ E2$
								L_1	78.20	0.7	50	0.62	0.037	0.13	0.41	
								M	85.46	0.3	60	0.27				
88.60	0.03	? $\surd$	0.03	···												
89.599	0.013		0.10	15												
90.720	0.015		0.04	···												
91.286	0.013		0.07	25												
91.407	0.013		0.09	20												
92.355	0.013		0.05	20												
92.819	0.015	?	0.05	···												
94.529	0.011		0.04	30												
94.643	0.011		0.20	15												
95.190	0.003	$\surd$	0.25	15	95.6	0.4	···									
95.767	0.003		0.09	10												
95.953	0.002		0.12	10												
96.265	0.020		0.02	30												
96.381	0.020		0.02	30												
97.253	0.020		0.015	···												
98.200	0.015		0.03	25												
98.572	0.016		0.04	20												

TABLE III. (*continued*).

I E_γ	II dE_γ	III	IV I_γ	V dI_γ	VI E	VII I	VIII dI	IX Shell	X E_e keV	XI I_e	XII dI_e	XIII α_{exp}	XIV $\alpha(E1)$	XIV $\alpha(E2)$	XIV $\alpha(M1)$	XV Multipolarity
98.8572	0.0015	√	0.56	10	99.5	0.33	···	L_1+L_2	89.46	0.3	60	0.60	0.034	0.75	0.31	$E2, M1$
99.293	0.014	?	0.015	···												
99.584	0.016		0.02	25												
102.55	0.04	?	0.016	···												
103.116	0.015		0.052	15												
104.295	0.015		0.049	15												
105.517	0.004	√	0.52	10				K	49.91	1.2	35	2.6	0.23	0.94	1.94	$M1+<30\%\ E2$
								L_1+L_2	96.12	0.14	60	0.30	0.028	0.57	0.26	
106.869	0.004		0.16	15												
107.181	0.016		0.04	20												
107.71	0.03		0.03	25												
108.199	0.002	√	0.85	10				L_1+L_2	98.80	0.2	50	0.26	0.027	0.51	0.24	$M1(+E2)$
109.241	0.012		0.03	20												
109.887	0.018		0.02	25												
110.327	0.012		0.04	20												
111.324	0.002	√	0.63	10				K	55.73	1.0	40	1.78	0.20	0.81	1.67	$M1(+E2)$
								L_1+L_2	101.95	0.2	50	0.36	0.025	0.45	0.22	
112.869	0.012		0.02	30												
113.17	0.02	?	0.02	···												
113.373	0.003		0.12	15												
113.644	0.004	√	0.15	15												
114.50	0.03		0.01	···												
115.167	0.004		0.09	15												
115.51	0.03		0.01	···												
115.759	0.003		0.34	15												
116.197	0.013		0.06	25												
116.835	0.001	√	15.8	10	117.4	12.6 *16*[a]	15 ···	K	61.22	19 *23*	15 *15*	1.34 *1.46*[c]	0.18	0.71	1.46	$M1+<3\%\ E2$
								L_1	107.44	2.9 *3.1*	15 *15*	0.20 *0.19*	0.018	0.067	0.18	
								L_2	107.92	*0.4*	*30*	*0.025*	0.0038	0.30	0.014	
								L_3		<0.2		*<0.012*	0.0046	0.29	0.0024	
								M	114.70	0.9	30	0.064				
								N	116.40	0.3	30	0.021				
117.264	0.003	√	0.20	10												
118.41	0.03		0.02	···												
118.49	0.02		0.03	···												
118.78	0.05		0.02	···												
120.06	0.02		0.02	30												
120.36	0.03	?	0.01	···												
121.48	0.03		0.01	···												
122.577	0.004	√	0.09	20												
122.89	0.02		0.01	···												
123.437	0.005	√	0.10	15												
123.81	0.02		0.01	···												
124.350	0.015		0.04	20												
126.228	0.003	√	1.06	10	126.9	1.8	···	K	70.62	0.7	30	0.74	0.14	0.57	1.17	$E2(+M1)$
								L_2	117.31	0.2	50	0.21	0.0030	0.21	0.0113	
								L_3	118.15	0.2	50	0.21	0.0035	0.19	0.0019	
128.566	0.005		0.14	15												
129.353	0.007		0.08	20												
130.641	0.016		0.01	···												
131.41	0.03		0.01	···												
131.759	0.005	√	0.14	15												
132.472	0.017		0.03	···												
134.00	0.03	? √	0.01	···												
134.34	0.03	√	0.02	30												
134.815	0.006		0.06	25												
135.15	0.02		0.04	30												
135.883	0.004		0.10	15												
136.662	0.002	√	27.5	10	137.4	21.7 *26*	15 *10*	K	81.05	2.8 *2.7*	15 *12*	0.114 *0.098*	0.117	0.46	0.94	$E1+<0.3\%\ M2$
								L_1+L_2	127.27	0.35 *0.30*	35 *18*	0.014 *0.011*	0.014	0.19	0.12	
137.09	0.03	?	0.01	···												
137.51	0.02		0.02	30												
137.99	0.04		0.007	···												
140.117	0.005		0.35	10				K	84.50	0.27	30	0.86	0.11	0.43	0.87	$M1(+E2)$
140.544	0.010		0.09	10												
141.599	0.007		0.13	10												
143.41	0.02		0.015	30												
145.00	0.03		0.02	···												
145.228	0.007		0.14	10												
146.808	0.008		0.095	15												

TABLE III. (*continued*).

I E_γ	II dE_γ	III	IV I_γ	V dI_γ	VI E	VII I	VIII dI	IX Shell	X E_e keV	XI I_e	XII dI_e	XIII α_{exp}	XIV $\alpha(E1)$	XIV $\alpha(E2)$	XIV $\alpha(M1)$	XV Multipolarity
149.307	0.003	√	4.25	10	149.9	3.44 *4.2*	15 *10*	K	93.70	2.9 *2.8*	25 *15*	0.68 *0.66*	0.093	0.36	0.73	$M1(+E2)$
								L_1	139.91	0.48 *0.4*	35 *25*	0.11 0.095	0.011	0.14	0.096	
150.268	0.008		0.11	15												
151.533	0.009		0.08	15												
152.45	0.03		0.016	30												
152.71	0.03		0.025	20												
153.32	0.04		0.006	···												
154.71	0.03		0.025	20												
155.42	0.03		0.025	20												
156.20	0.03		0.014	···												
156.45	0.03		0.014	···												
157.344	0.008	√	0.21	15												
157.95	0.05		0.014	···												
158.702	0.009	√	0.06	20												
159.38	0.02		0.05	20												
159.89	0.03		0.01	30												
160.63	0.02		0.04	20												
161.42	0.02		0.03	20												
162.452	0.010		0.065	20												
163.352	0.007		0.51	10	163.7	0.4	30									
164.57	0.04		0.02	30												
166.983	0.005		0.17	10												
167.450	0.005		0.95	10	168.6	*1.7* 0.76	*15* 15	K		<0.18		<0.19	0.069	0.26	0.53	$E1$
168.49	0.03		0.04	30												
169.45	0.03		0.02	···												
169.712	0.005		0.24	10												
170.09	0.03		0.01	···												
170.584	0.015		0.05	20												
171.67	0.03	√	0.03	20												
173.47	0.12	*c*	0.02	···												
174.77	0.04		0.02	···												
175.73	0.04		0.03	30												
175.98	0.02	√	0.07	20												
177.71	0.04		0.01	···												
179.032	0.006		0.25	15				K	123.42	0.12 *0.15*	60 *30*	0.32 *0.60*	0.058	0.22	0.44	$M1(+E2)$
179.882	0.004	√	0.25	15				K	124.27	0.12 *0.15*	60 *30*	0.32 *0.60*	0.057	0.21	0.43	$M1(+E2)$
180.545	0.005		0.20	15				K	124.93	0.12 *0.08*	60 *40*	0.40 *0.40*	0.056	0.21	0.43	$M1(+E2)$
181.086	0.005	√	1.27	10	181.5	*2.2* 1.68	*12* 15	K	125.48	0.79 *0.55*	30 *20*	0.42 *0.43*	0.056	0.21	0.42	$M1(+E2)$
								L_1+L_2	171.69	0.12	60	0.064	0.0068	0.063	0.056	
182.04	0.04		0.02	···												
182.302	0.016		0.10	15												
183.11	0.06	?	0.01	···												
183.96	0.04		0.05	30												
184.23	0.02		0.15	10												
186.147	0.006	√	0.12	15												
186.582	0.006		0.28	10	186.7	0.48	20	K	130.97	0.1	70	0.24	0.052	0.19	0.39	$M1$, $E2$
187.93	0.05		0.01	···												
188.98	0.03	*c*	0.07	20												
189.89	0.05		0.01	···												
191.12	0.03		0.03	20												
191.961	0.011		0.13	15												
192.33	0.02		0.07	20												
193.107	0.006	√	0.19	10												
194.529	0.010		0.13	15	194.3	0.33	30									
195.687	0.014		0.08	15												
197.11	0.05		0.03	···												
197.339	0.008	√	0.32	15				K	141.73	0.12	60	0.26	0.045	0.16	0.33	$M1$, $E2$
197.677	0.010		0.20	15												
198.31	0.05		0.03	···												
199.12	0.05		0.04	30												
199.710	0.008	√	0.80	10	199.8	*1.4* 1.0	*15* 15	K	144.10	0.31	35	0.26	0.043	0.16	0.32	$M1(+E2)$
201.08	0.03		0.04	20												
201.95	0.03		0.05	20												
205.03	0.08		0.02	···												
206.15	0.02		0.05	15												
207.04	0.02	√	0.04	15												

TABLE III. (*continued*).

I E_γ	II dE_γ	III	IV I_γ	V dI_γ	VI E	VII I	VIII dI	IX Shell	X E_e keV	XI I_e	XII dI_e	XIII α_{exp}	XIV $\alpha(E1)$	XIV $\alpha(E2)$	XIV $\alpha(M1)$	XV Multipolarity
208.34	0.04		0.065	15												
208.90	0.04	√	0.03	20												
209.69	0.04		0.02	30												
210.300	0.006	√	0.30	15				K	154.69	0.18	50	0.4	0.038	0.14	0.28	$M1(+E2)$
211.06	0.06		0.03	20												
211.53	0.06		0.01	···												
212.30	0.06		0.04	20												
213.04	0.06		0.01	···												
214.442	0.009		0.22	15	215.7	0.2	···	K	158.83	0.14	60	0.4	0.036	0.13	0.26	$M1(+E2)$
215.44	0.09	?	0.01	···												
216.16	0.05	√	0.02	30												
216.85	0.06		0.04	···												
217.23	0.06		0.04	···												
218.00	0.06		0.04	···												
219.02	0.06		0.06	30												
219.44	0.06		0.08	25												
221.174	0.009	√	3.9	10	222.5	*3.2* *3.7*	15 *10*	K	165.56	*1.3* *0.83*	35 *12*	0.22 *0.21*	0.033	0.12	0.24	$M1(+E2)$
								L_1+L_2	211.78	*0.27* *0.14*	60 *20*	0.05 *0.036*	0.0041	0.030	0.032	
222.634	0.007		0.22	10												
224.01	0.15	?	0.01	···												
225.722	0.009		0.07	20												
227.88	0.07	c √	0.02	···												
228.53	0.07		0.05	30												
229.00	0.07	√	0.05	30												
230.11	0.05		0.03	20												
230.89	0.08		0.03	20												
231.957	0.014		0.24	20												
232.286	0.009		0.27	20												
233.112	0.014		0.63	10	234.1	*1.2* 1.18	*20* 15	K	177.50	0.24	35	0.26	0.029	0.10	0.21	$M1(+E2)$
233.79	0.05		0.12	20												
234.79	0.05		0.05	···												
235.80	0.05		0.06	30												
236.31	0.08		0.03	30												
239.140	0.011	√	4.2	10	240.2	*3.4* *4.0*	15 *12*	K	183.53	*1.1* *0.78*	35 *12*	0.17 *0.18*	0.027	0.095	0.20	$M1(+E2)$
								L_1+L_2	229.74	0.2	50	0.03	0.0033	0.023	0.026	
241.76	0.05		0.05	20												
242.90	0.02		0.17	20												
245.007	0.007		1.04	10	246.2	1.1	15	K	189.40	0.27	35	0.17	0.026	0.089	0.18	$M1(+E2)$
246.07	0.02		0.20	20												
247.68	0.09		0.03	30												
248.77	0.09		0.06	20												
250.49	0.09		0.07	20												
253.78	0.03		0.12	20												
255.37	0.03		0.09	20												
256.60	0.02		0.26	15				K	200.99	0.09	70	0.24	0.023	0.078	0.16	$M1(+E2)$
257.81	0.02		0.26	15	258.5	0 5	···	K	202.20	0.21	60	0.5	0.023	0.077	0.16	$M2(+E1)$
260.75	0.02		0.16	15												
261.31	0.07		0.04	30												
261.96	0.07		0.05	···												
262.93	0.09	?	0.3	···												
263.36	0.05		0.12	15												
265.12	0.05		0.18	20												
266.03	0.05		0.28	20												
266.53	0.05		0.24	20	267.6	0.55	20									
267.19	0.05		0.28	20												
267.82	0.09		0.11	20												
268.15	0.09		0.07	30												
269.38	0.09		0.07	30												
273.64	0.07		0.16	20												
274.77	0.07		0.13	20												
276.83	0.02		0.03	···												
278.69	0.10	c	0.06	30												
279.79	0.10		0.03	30												
280.99	0.10		0.03	30												
282.80	0.08		0.06	30												
284.26	0.12		0.08	30												
285.81	0.08		0.06	30												
287.24	0.03	√	0.17	15												
288.60	0.07		0.12	···												
289.120	0.015	√	2.3	10	289.2	1.04	30	K		<0.09		<0.03	0.017	0.055	0.117	$E1$
290.61	0.03	√	1.7	10	291.3	3.0	30	K	235.00	0.24	40	0.10	0.017	0.055	0.117	$M1(+E2)$

TABLE III. (*continued*).

I E_γ	II dE_γ	III	IV I_γ	V dI_γ	VI E	VII I	VIII dI	IX Shell	X E_e keV	XI I_e	XII dI_e	XIII α_{exp}	XIV $\alpha(E1)$	XIV $\alpha(E2)$	XIV $\alpha(M1)$	XV Multipolarity
291.04	0.08		0.12	···												
293.42	0.08		0.07	20												
295.99	0.08		0.04	30												
297.90	0.03	√	0.39	20	298.4	0.4	20	K	242.29	0.09	60	0.15	0.016	0.051	0.11	$M1(+E2)$
299.88	0.17		0.03	···												
304.60	0.02		2.6	10	305.7	2.2	12	K	248.99	0.35	35	0.09	0.015	0.048	0.10	$M1(+E2)$
								L_1+L_2	295.20	0.09	70	0.02	0.0018	0.010	0.013	
306.49	0.03		0.24	20												
307.65	0.15	?	0.03	···												
309.59	0.06		0.10	20												
310.89	0.03		0.30	15	311.9	0.4	20									
312.90	0.08		0.12	30												
313.48	0.06		0.12	30												
316.10	0.09		0.09	···												
317.28	0.03		0.22	15	317.14	0.17	30									
321.62	0.10	?	0.09	···												
323.42	0.07		0.12	20												
324.74	0.07		0.11	20												
328.245	0.015		0.73	10	329.3	0.53	20									
331.88	0.03		0.27	15												
333.62	0.02		1.6	15	334.2	1.16	15	K	278.01	0.19	50	0.08	0.012	0.037	0.080	$M1(+E2)$
335.61	0.08		0.62	20	337.1	0.32	25									
338.20	0.04		0.15	15												
341.57	0.03		0.28	20												
343.51	0.03	√	0.39	20	344.1	0.34	15									
347.24	0.08		0.20	20												
350.61	0.12		0.07	20												
352.28	0.12		0.13	20	352.1	0.08	···									
357.04	0.04	√	0.29	20	358.1	0.19	30									
358.4	0.3		0.05	···												
359.7	0.2		0.08	30												
363.1	0.3		0.05	···												
367.54	0.16	√	0.07	···	367.0	0.06	···									
368.45	0.16		0.12	25												
371.75	0.03	√	3.0	10	372.5	2.69	12	K		<0.07		<0.016	0.009	0.028	0.060	$E1$
373.47	0.07		0.45	15												
376.91	0.14		0.12	20												
380.1	0.2		0.05	30												
382.8	0.2		0.05	···												
385.0	0.2		0.04	···												
386.3	0.3		0.04	···												
390.0	0.2		0.18	20												
391.89	0.04		1.13	10	391.5	0.57	···									
394.5	0.2		0.10	···	393.0	0.55	···									
398.6	0.2		0.09	30												
401.56	0.06		2.10	15	402.0	1.74	10	K	345.95	0.12	70	0.03	0.0075	0.022	0.049	$M1, E2$
406.83	0.16		0.13	20	407.9	0.3	···									
410.27	0.02		1.36	20	411.3	2.16	10									
411.09	0.03		0.75	30												
412.1	0.2		0.60	20												
413.69	0.15		0.15	···												
416.47	0.05		0.8	20	416.3	0.86	20									
418.08	0.18		0.2	30												
421.13	0.05		0.7	15	421.2	0.69	30									
423.39	0.18		0.16	···												
425.30	0.03	√	1.3	20												
425.99	0.03		3.7	15	425.8	3.2	25									
427.0	0.2		0.4	···	427.2	1.7	30									
430.31	0.18		0.13	···												
432.14	0.18		0.13	···	432.5	0.4	30									
433.92	0.18		0.17	···												
437.3	0.3		0.06	···	436.1	0.2	···									
439.6	0.3		0.04	···												
442.0	0.3		0.4	30	441.8	0.6	15									
442.9	0.3		0.4	30												
450.3	0.3		0.05	···												
454.96	0.20		0.3	···	454.0	0.9	30									
455.60	0.06		1.7	15	456.6	0.8	30	K	399.99	0.07	60	0.03	0.0056	0.016	0.036	$M1(+E2)$
457.37	0.07		0.6	20												
463.9	0.3		0.6	20	462.8	0.5	25									
467.3	0.3		0.3	30	466.9	0.4	30									
472.2	0.5		0.14	···	472.0	0.6	30									
475.8	0.3	?	0.15	···	476.0	1.1	30									

TABLE III. (*continued*).

I E_γ	II dE_γ	III	IV I_γ	V dI_γ	VI E	VII I	VIII dI	IX Shell	X E_e keV	XI I_e	XII dI_e	XIII α_{exp}	XIV $\alpha(E1)$	XIV $\alpha(E2)$	XIV $\alpha(M1)$	XV Multipolarity
477.4	0.3		0.2	···												
481.31	0.08	*c*	0.85	20	480.1	1.4	20									
487.58	0.06		1.3	15	484.7	0.7	30									
489.39	0.05		3.2	10	488.2	2.2	20	*K*	433.78	0.09	60	0.02	0.0048	0.013	0.030	*E2*, *M1*
496.9	0.2		0.3	···	493.6	0.4	···									
499.5	0.4	*c*	0.1	···	497.5	0.4	···									
504.3	0.2		0.2	···	504.4	0.4	···									
506.8	0.3	?	0.2	···												
509.0	0.2		0.7	···	508.5	1.3	30									
510.9[b]	0.3		0.8	20	511.4	1.1	30									
512.7	0.3		0.8	20												
524.2	0.3		0.5	20	522.3	0.6	···									
530.1	0.3		0.4	···	531.0	0.5	···									
533.5	0.3		0.6	30												
534.9	0.4		0.3	···	535.4	0.5	···									
538.4	0.3		0.3	···												
542.86	0.20		3.5	25	540.4	2.9	···	*K*	487.48	0.15	40					
543.66	0.20		2.4	25	542.5	1.9	···									
550.5	0.3		0.3	···	548.0	0.5	···									
554.3	0.4		0.6	···	551.8	0.55	25									
564.8	0.3		0.2	···												
570.0	0.3		0.2	···												
577.0	0.3		0.7	20												
585.6	0.7		0.4	30												
589.4	0.7		0.3	30												
593.8	0.7	?	0.08	···												
600.8	0.7		0.3	···												
607.7	0.7		0.11	···												
612.0	0.5		0.3	···												
613.8	0.4		0.7	30												
618.5	0.7		0.3	···												
624.0	0.4		0.6	30												
633.5	0.4		0.8	30												
643.1	0.8		0.4	30												
653.4	0.8		0.2	···												
658.9	0.6		0.6	30												
661.0	0.6		0.6	30												
681.7	0.5		0.4	30												
689.7	0.9		0.8	30												
699.4	0.9		0.5	30												
708.9	0.6		0.3	···												
715.3	0.6		0.6	30												
734.4	1.0		0.3	···												

[a] Normalization value. See Sec. IIIC. [b] Annihilation radiation. [c] Normalization value. See Sec. IIIE.

ment of the spectrometer, the absolute γ intensities $I_\gamma/100n$ (γ quanta per 100 captured neutrons), and the relative intensity errors dI_γ/I_γ are given in Table III. The energies E_γ are not absolute energies (in keV). Since the absolute energies of the $K\alpha_{1-}$ and $K\alpha_{2-}$ lines of holmium x radiation as given by Bergvall[50] have been used to calibrate the spectrometer, the ratio between our relative energy values and the absolute energies of the transitions (in keV) is 1.00000 ± 0.00002. The difference between absolute and relative energies is important because our relative energy errors include neither the errors of Bergvall's values,[50] nor our calibration error. It may seem confusing to quote relative energies instead of absolute values; however, as we shall see in greater detail in the discussion, the maximum precision of the relative numbers is required and relevant in analyzing the data.

The intensities I_γ have been obtained from relative intensities and a comparison of these numbers with the absolute values for a few strong transitions which had been measured by Orecher.[26] An independent computation of the absolute intensities was performed by comparing the relative γ intensity of the 80.6-keV transition in Er^{166} (which was produced during the β decay of the 27.7-h ground state of Ho^{166}) with the absolute transition intensity determined by Graham *et al.*[6] Details have been described elsewhere.[20]

The diffraction spectrometer is subject to occasional undeterminable intensity errors due to the fact that the source can move and affect the transmitted intensity. In order to ensure that the γ-ray intensities are reliable, two independent experiments were performed with lithium-drifted germanium detectors: (i) an external neutron beam, using a liquid-nitrogen-cooled quartz filter and lead-crystal filter, was used at Studsvik with a 90-deg position detector and (ii) the Los Alamos facility used in making the high-energy measurements was used with the annulus in anticoincidence to accentuate the

[50] P. Bergvall, Arkiv Fysik **16**, 57 (1959).

total energy peaks [see Fig. 4(b)]. The interpretation of intensities from such spectra can only be performed when the high-resolution data from Risø is available to allow the interpretation of areas from "peaks" to be confidently interpreted as due to a single γ ray or in some cases to unresolved doublets or triplets. This has been done at Studsvik from 116 to 239 keV and at Los Alamos from 70 to 550 keV. The Studsvik arrangement was calibrated with the known intensities from a radioactive source of Ta^{182}. The measured relative intensities were compared to that of the 116.835-keV γ ray. The Los Alamos measurements were performed on an absolute partial cross section basis from 116 to 537 keV by intercomparison with the known thermal cross section for the 411-keV γ ray from a gold sample. Only target mass and timing ratios enter into this scheme along with absorption corrections. In addition, the lines from 70 to 100 keV, insofar as they could be properly integrated, were compared with the known intensity of the 80.6-keV Er^{166} line from the 27.7-h β decay of Ho^{166} to Er^{166}. Self-absorption corrections, which became severe in comparison with the several-hundred-keV region, were virtually eliminated in this measurement. The radioactive decay strength was determined by merely lowering the thermal column curtain which attenuates the thermal neutrons (and thus the prompt capture) by a factor of about 700. These two experiments agree within about 20%.

D. The β Decay of Dy^{166}

In order to gain the maximum possible knowledge about low-lying states in Ho^{166}, the γ radiation emitted during the Dy^{166} decay has also been measured with the crystal spectrometer at Risø. Apart from the transitions observed previously, the 290-keV line which has been observed before by Helmer[1] in a coincidence spectrum only, has been detected and measured in the singles γ spectrum.[51] Its energy has been determined as 290.66 $\pm$0.10 keV (see Table VI) and its intensity was found to be 2.3×10^{-2} ($\pm$20%) times the intensity of the 425.99-keV line.

E. The (n,e^-) Spectrum

The conversion electrons of Ho^{166} from neutron capture in Ho^{165} have been measured in these experiments with two different β-ray spectrometers: the Elephant spectrometer[52] at the *FRM* reactor in Munich with the target close to the core, and the Studsvik β spectrometer,[53] where a neutron beam from the R2 reactor impinges on a target in the spectrometer which is located outside the reactor.

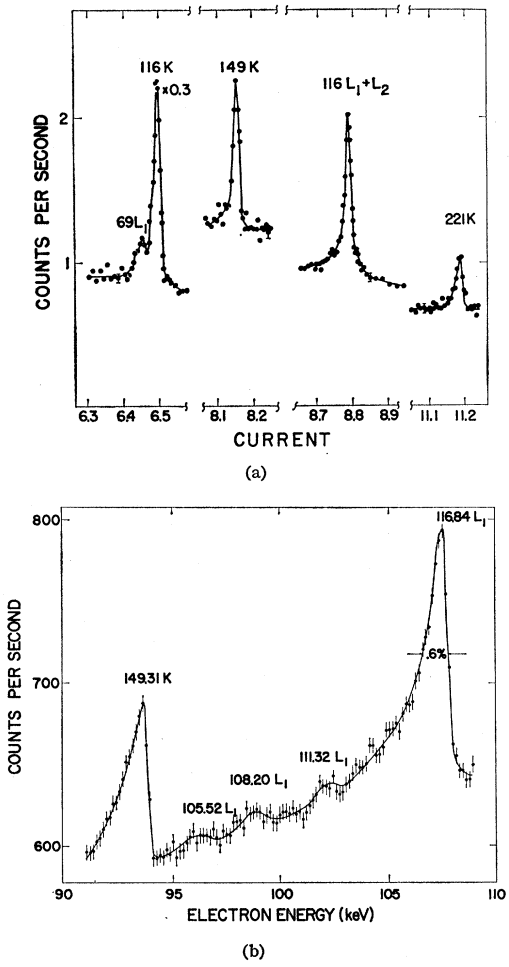

FIG. 5. (a) Part of the conversion electron spectrum of Ho^{166} measured with the double-focusing spectrometer at Studsvik using an external beam of neutrons from the R-2 reactor. The resolution (FWHM) was better than 0.3%; (b) part of the conversion electron spectrum of Ho^{166} measured with the "Elephant spectrometer" at the FRM reactor near Munich.

The measurements at Munich were done with a relatively thick source which aided in the observation of a large number of electron lines. However, the precise determination of electron intensities was difficult because of the presence of tails on the low-energy side of lines especially below 100-keV electron energy. The thinner source used at Studsvik allowed a more accurate determination of intensities although fewer lines were observed. This proved particularly important in normalizing the Munich data at higher energies. Portions of the Studsvik and Munich data are shown in Figs. 5(a) and (b).

[51] Recently, this line has also been observed by D. Hafemeister and E. Brooks Shera, using a lithium-drifted germanium detector at the Los Alamos Scientific Laboratory. Their result is in good agreement with our data. We are grateful to Dr. Hafemeister and Dr. Shera for kindly communicating their result to us.

[52] T. v. Egidy, Ann. Physik **9**, 221 (1962); E. Bieber, T. v. Egidy, and O. W. B. Schult, Z. Physik **170**, 465 (1962); W. Nörenberg, Z. Angew. Phys. **17**, 452 (1964); E. Bieber, Z. Physik **189**, 217 (1966).

[53] G. Bäckström, A. Bäcklin, N. E. Holmberg, and K. E. Bergkvist, Nucl. Instr. **16**, 199 (1962) and A. Bäcklin (to be published).

1. Measurements at Studsvik

Some of the stronger internal conversion lines were measured with the double-focusing spectrometer at Studsvik. This instrument is a conventional 50-cm radius spectrometer of the Siegbahn-Svartholm type located at a beam hole in the Studsvik R2 reactor. A neutron beam is extracted from the reactor into the spectrometer, giving a neutron flux density at the source position inside the spectrometer of 10^8 (thermal neutrons)/cm^2 sec. The spectrometer is normally adjusted to give a resolution of 0.2% (FWHM).

A source arrangement due to Bergkvist[53] is used in the spectrometer. The source material is deposited on 20 parallel strips of aluminum foil, 1.5 mm×50 mm, which are connected to equidistant taps in a voltage divider. By applying a suitable high tension, the images of all the strips can be made to coincide at the detector slit. This arrangement makes it possible to utilize the full width of the neutron beam, thereby increasing the luminosity of the spectrometer more than an order of magnitude with a retained resolution of 0.2%. Further details concerning the instrument are given in Ref. 53.

A comparatively thin source was preferred in order to minimize the systematic error in the intensity determination that may be caused by a strongly energy-dependent resolution and low-energy "tail" of the lines. To a certain extent these effects may be compensated for by using the area under a line as a measure of the intensity. However, when the source is so thick that an appreciable part of the area of the line is contained in the low-energy "tail," this method is unreliable because of the great difficulty in separating the "tail" from the background. The source of approximately 0.1 mg/cm^2 thickness was prepared by evaporating metallic holmium on aluminum backing of a thickness of 3 mg/cm^2. The contribution to the linewidth due to the source thickness was negligible above 100-keV electron energy. Below that energy some broadening was observed, but it was less than 0.1% for all lines.

The result of the measurements is given in Table III. All lines were recorded at least three times. Good agreement was found between the results of the different recordings. Some examples of the recorded lines are shown in Fig. 5(a). As the neutron flux from the reactor showed a good short-time stability, it was not necessary to monitor the neutron flux from the reactor during the time of each recording. However, the long time variations of the flux were found to be considerable, so, in order to normalize the recordings to each other, the 116-keV K line was measured at the beginning of each run.

Conversion coefficients were calculated with the aid of the Risø γ-ray intensities of Table III. Both the K/L ratio and the L_1/L_3 ratio of the 116-keV transition are compatible with a pure $M1$ transition with a maximum of 3% $E2$ admixture. In order to normalize the conversion coefficients, the conversion coefficient of the 116-keV transition was assumed to have the theoretical value for a pure $M1$ transition.[54] From the K-conversion coefficient of the 136-keV transition, the $M2$ admixture is found to be less than 0.3%.

2. Measurements at Munich

The source at the *FRM* spectrometer consisted of 0.6 mg/cm^2 of holmium metal evaporated on a 0.2 mg/cm^2 aluminum backing. Its size was 80 mm×12 mm. The size of the slit in front of the detector was chosen as 10 mm×1.5 mm corresponding to the focusing properties of the magnet which yields a scale ratio 8:1. The linewidth (FWHM) was approximately 0.6% at 100 keV and 0.3% at 200 keV because of the target thickness. The number of electrons was counted for 1 min in each of the 2600 magnet field settings in the energy range from 28 keV to 550 keV. A few lines were measured for 5- or 10-min intervals. The conversion-electron data involving the relative electron intensities are contained in Table III. The Munich electron data are calibrated up to 150-keV γ-ray energy on the basis that the 116- and 136-keV gamma rays are pure $M1$ and $E1$ transitions. The assumption of pure multipolarities is quantitatively justified by the Studsvik data presented in Table III. These two γ rays furnish three experimental calibration points: the 116-keV K and L_1 lines and the 136-keV K line with respect to the theoretical conversion coefficients. The Munich experimental average ratio of electron to γ-ray intensity for these three electron lines is normalized to the average of the theoretical conversion coefficients to determine the normalization factor for the calibration. Above 175 keV the experimental values of the thin source Studsvik conversion coefficient are used for the normalization factor. The K lines of the 181-, 221-, and 239-keV transitions are averaged to give the new calibration constant. In this way the difficulties inherent in the thick source used to observe electron lines in the Munich experiment were overcome.

Additional information about the multipole order of the transitions can be gained from Fig. 6 which shows the energy dependence of the sensitivity of the Elephant spectrometer for electron lines expected from conversion of γ radiation of multipole order $E1$, $M1$, and $E2$ in different atomic shells. The curves follow from the absorption of low-energy electrons in the counter window, from the target thickness, from the background and from the theoretical conversion coefficients.[55] The points in Fig. 6 correspond to γ-ray energy on a log-log scale. Conversion electron lines have been observed for those gamma transitions which are shown as triangles.

---

[54] M. E. Rose, *Internal Conversion Coefficients* (North-Holland Publishing Company, Amsterdam, 1958).

[55] L. S. Sliv and I. M. Band, *Coefficients of the Internal Conversion of Gamma Radiation* (Academy of Science of the USSR, Moscow, 1956).

F. Population of the 1200-Year Isomer

A separate experiment was performed to determine the fraction of the absorption cross section in Ho^{165} which leads to the 1200-year[12] 7− level in Ho^{166}. In this experiment, a 94.3 mg source of Ho_2O_3 was irradiated for 37.7 h in the thermal column of the Omega West Reactor and, after a delay of 31 days when the 27.7-h activity had decayed to $<10^{-8}$ of its initial intensity, a fresh irradiation of an 8.1 mg source was made for 35 sec in the same flux. The intensity of the 27.7-h 80.6-keV activity was then compared with the intensities of the 1200-year 80.6-keV and 184-keV intensities in a 3 in.×3 in. NaI scintillator. The 80.6 keV-line intensity was clearly identified for both sources.

The intensity of the 80.6-keV γ ray is reported by Cline *et al.*[56] to be (6.7±0.5) percent of the decay rate of the 27-h ground state in Ho^{166}. Also Cline and Reich[11,57] observed that 11.6% of the decays of the 1200-year isomer result in an 80.6 keV γ ray and 90.4% result in an 184-keV γ ray. We thus find by comparing the intensity of the 80.6-keV lines from the two sources that $\sigma_c(1200\text{-year})/\sigma_c(27.7\text{-h})=0.056\pm0.010$, and by comparing the 80.6-keV and 184-keV intensities, that $\sigma_c(1200\text{-year})/\sigma_c(27.7\text{-h})=0.053\pm0.010$. The average of the two ratios is 0.055±0.007. Taking the absorption cross section of Ho^{165} to be 66.5±3.3 b,[20] the cross section for populating the two levels is 63±3.2 b (27.7-h) and 3.5±0.5 b (1200-year).

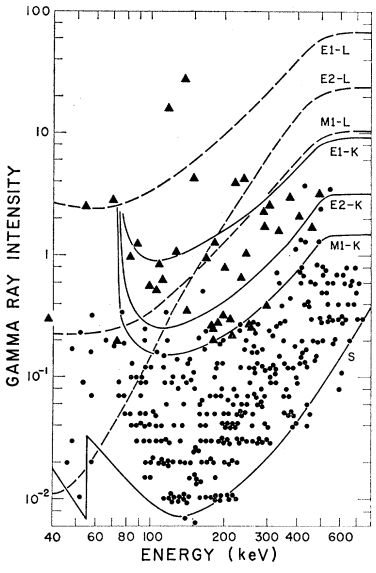

FIG. 6. Log-log plot of the low-energy neutron capture γ-transitions of Ho^{166}. The curve S corresponds to the sensitivity limit of the Risø curved crystal spectrometer (see Appendix A). The other curves indicate sensitivity limits of the "Elephant spectrometer" for the detection of electron lines from internal conversion in different atomic shells. Triangles correspond to transitions for which the conversion electron line intensities have been measured. Points correspond to all other measured low-energy γ rays as listed in Table III.

[56] J. E. Cline, E. C. Yates, and E. H. Turk, Nucl. Phys. **30**, 154 (1962).
[57] C. W. Reich and J. E. Cline, Phys. Rev. **137**, B1424 (1965).

IV. DISCUSSION

Struble *et al.*[17] have interpreted the low-lying levels of Ho^{166} excited in the (d,p) process as rotational states superimposed on two-quasiparticle states obtained from the lowest possible Nilsson configuration of the 67th proton and the 99th neutron. For this reason, it might seem tempting to fit the data obtained during the experiments described in this paper simply into Struble's level scheme. However, we believe that more insight into the nuclear structure of the Ho^{166} levels is gained if we construct our level scheme independently of Struble's work. In those cases where our data are insufficient for an extension of our scheme, we will, of course, compare them with Struble's diagram in order to see whether or not our data and Struble's results are consistent.

It is usually difficult or even—within our present limitation of experimental techniques—impossible to unambiguously prove every detail of a very complex nuclear level scheme through experiment. This is particularly true when the interest is focused on details of the nuclear structure of the states. The experimentalist then often uses theoretical models which hopefully facilitate the construction of the nuclear level scheme. Then, however, the question arises whether the experiment proves the scheme completely independently of the model on the one extreme, or, on the other whether the experiment proves nothing while being completely consistent with a theoretical scheme or model. In this latter case, it is necessary to make sure that the model chosen is the only one consistent with the data. Otherwise, the data support the model, but they do not uniquely prove it. The usual situation is somewhere between these extremes. Thus, it is important to clearly state what is proved and what has been assumed. Proved features used together with assumptions may lead to a conclusion in which it finally is impossible to quote exactly the extent to which a particular feature in the level scheme has been proved and to which extent assumed.

Well aware of these difficulties, we will try to construct the level scheme of Ho^{166} as far as possible without using a theoretical model. The assumptions we make will be explicitly stated. After the level scheme has been established, it will be compared with a theoretical model. The quality of the agreement between experiment and theory will then tell us how well the structure of the nucleus can be understood in terms of the chosen model.

A. The Ground-State Rotational Band

A comparison of our low-energy γ transitions with the results from the investigation of the Dy^{166} decay unambiguously shows that our strong 54.239-keV line is the 2− → 0− transition and that the 82.470-keV

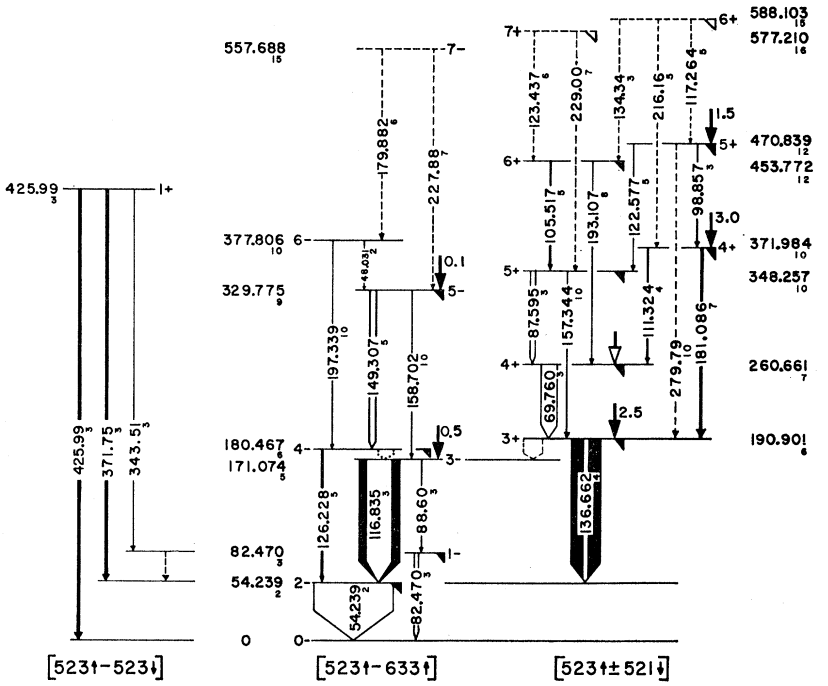

FIG. 7. Nuclear level scheme of Ho^{166}. The experimental evidence for the dashed levels is not sufficient for an unambiguous assignment of these states. The energies and energy errors given in this scheme are absolute values (keV). Conversion electron transitions are given as white areas of arrows limited at both sides by dark lines the total width of which is proportional to the γ intensity. A short thick vertical arrow leading into a level indicates feeding of this state through a high-energy γ transition directly from the compound state. An open arrow indicates that the high-energy population through a primary transition is uncertain. The intensity of the transition (γ's per 1000 neutrons captured) is written beside the arrow. A triangle directed downwards at the right end of a level indicated that the state has been observed in the (d,p) reaction.

radiation corresponds to the $1- \rightarrow 0-$ transition. In addition, our conversion electron data yield multipolarities for these lines in agreement with the assignments obtained from decay studies.[1,2] The multipolarity of the intense γ ray at 116.8 keV has been found to be $M1$ with less than 3% $E2$ which agrees with previous measurements.[20,30] The total intensity ($I_\gamma+I_{e-}$) of this 116.8-keV line requires that it feed the 54.2-keV level. Any other possibility is excluded. We thus obtain a level at 171.074 keV with negative parity and spin 1, 2, or 3. This state also decays through a rather weak transition to the 1− state at 82.47 keV. Assuming reasonable transition probabilities throughout this work, the absence of a line from the 171.0-keV level to the 0− state requires spin parity 3− for the 171-keV level. This assignment as well as the energy of the state is in good agreement with the observation of a high-energy transition from the compound state to a level at 170.8±0.8 keV.

A further state at 330±3 keV is found through another high-energy (n,γ) primary transition. This state is also obtained from the low-energy (n,γ) data through a well-satisfied energy combination where four transitions are involved (see Fig. 7 and the first line of Table X, Appendix A). This quadruple combination yields states at 329.77 and 180.467 keV. The 180-keV level is preferred over the other value offered by the inversion of the 149- and 126-keV lines because of better agreement with the (d,p) results and later construction of the decay scheme. This level is then depopulated through the 126.228-keV transition to the 2− state at 54 keV. Spin parity 4− is found for the 180.467-keV level because of the probable multipolarity ($E2$) of the 126-keV line and the fact that no transitions to the 0-keV (0−) and 82.4-keV (1−) states have been seen. The total intensity of the 149.3-keV transition exceeds that of the 126.2-keV transition and requires a 9.39-keV transition from the 180.4 keV (4−) state to the 171.0-keV level (3−).

The population of the 329.775-keV level through a direct high-energy transition, the absence of transitions to the 0−, 1− and 2− states and the measured multipole order (predominantly $M1$) of the 149-keV line, require spin parity 5− for the 329-keV level.

The energy of the 149-keV transition is reproduced within 1 eV by the difference of the 197.339±0.010-keV line and the 48.031±0.002-keV transition. The resulting state at 377.806 keV has negative parity because of the measured $E2$ multipolarity of the 197-keV transition. No transitions to the 0−, 1−, 2−, and 3− levels have been observed. The 377-keV level is therefore a 6− state, the total population of which is in agreement with what is expected from general population considerations.[58]

Thus, we obtain from the exclusive use of our neutron capture data levels with spins and parity 3−, 4−, 5−, and 6−. The only assumption we have made was: reasonable transition probabilities. Our experiments prove the existence of the corresponding 3−, 4−, and 5− levels which have been proposed previously[17] as a result of (d,p) data using an extension of the collective model.

We may now proceed by comparing our result with theory. If the rotational model applies, one can expect

[58] O. W. B. Schult, B. P. Maier, H. R. Koch, and U. Gruber, Z. Physik **185**, 295 (1965).

in the particular case of a $K=0-$ band, two rotational bands, one containing the even members, the other containing the odd members only.[59] Using the 0^- to 5^- members of these bands, we find, using[60]

$$E=E_0+AI(I+1)+BI^2(I+1)^2, \quad (4)$$

for the even I members: $E_0=0$ keV,

$$A_{\text{even}}=9.0470 \text{ keV}\pm 0.3 \text{ eV},$$

and

$$B_{\text{even}}=-1.18 \text{ eV}\pm 0.02 \text{ eV},$$

and for the odd members:

$$E_0=64.712 \text{ keV}\pm 3 \text{ eV},$$

$$A_{\text{odd}}=8.8823 \text{ keV}\pm 0.3 \text{ eV},$$

and

$$B_{\text{odd}}=-1.56 \text{ eV}\pm 0.02 \text{ eV}.$$

The difference in the rotational parameter E_0 for the even and odd members of the $K=0-$ band indicate to what extent this band is split into two separate bands. Using the rotational formula as given above, a value of $E(\text{theory})=197.424$ keV$\pm$35 eV is calculated for the distance between the 6− and 4− levels, a number which is very close to the experimental value $E(\text{exp.})=197.339$ keV$\pm$10 keV.

The rotational model predicts the difference between the 7− and 5− levels as $E_{\text{cal}}=227.450$ keV$\pm$60 eV. A complex line at about 227.88 keV is observed in the low energy (n,γ) spectrum and combines with the 48.031-keV line and the 179.883-keV $M1$ transition yielding $E(\text{exp.})=227.913$ keV$\pm$7 eV for the distance from 7− to 5− and a negative parity state at 557.688 keV. Since accidental combinations with weak lines such as the 227.88-keV complex are frequent (see discussion in Appendix A), the fit of the energy combination is necessary for the existence of a state, but it is not sufficient. For this reason, we consider the fit of the combination in this case not to be strong enough evidence for the existence of the state at 557.6 keV. Population considerations[58] indicate that the spin of the 557-keV state should be larger than 6, which together with the $M1$ character of the 179-keV line would require spin 7− for this level.

In addition to the familiar level energy sequence, we expect characteristic features for the branching ratio within a rotational band. In an odd-A nucleus, for instance, the quadrupole moment Q and the term $K^2(g_K-g_R)^2$ should be fairly constant. We assume that we can express the reduced transition probabilities within a rotational band in Ho^{166} in analogy to the odd-A case as

$$B(E2, I_i\rightarrow I_f)=[5/16\pi]e^2q^2 \times 10^{-48} \text{ cm}^4\langle I_i 2K0|I_i 2I_f K\rangle^2 \quad (5)$$

and

$$B(M1, I_i\rightarrow I_f)=[3/4\pi](e\hbar/2M_pc)^2C^2 \times\langle I_i 1K0|I_i 1I_f K\rangle^2. \quad (6)$$

q corresponds to the quadrupole moment expressed in barns and C is analogous with $K(g_K-g_R)$ in the odd-A case.[31] The ratio C^2/q^2 has been calculated several times using the observed γ intensities of the transitions within the $K=0$ band in Ho^{166} (see Table IV). In these calculations, transitions between states with spins I and $I-1$ have been considered to be pure $M1$ transitions as is to be expected within an unmixed $K=0$ band, because the Clebsch-Gordan coefficients vanish then for $E2$ components. Table IV shows that the ratio C^2/q^2 is constant within the experimental error. This indicates that all the states involved belong to one family as is predicted by the collective model. Since the 227.8-keV line is complex, only a lower limit for C^2/q^2 can be given. Yet, the number obtained fits nicely among the others, supporting the assumption that the 557-keV level is the 7− member of the ground-state rotational band. Assuming a quadrupole moment of 8 b, we obtain on the average that $C^2=20$ which means that the $M1$ transitions in the $K=0$ band are quite fast. The interpretation of the ground-state band as a $K=0$ band with rotational states superimposed on the $[523\uparrow-633\uparrow]$ configuration is consistent with the experimental data.

TABLE IV. γ-transition strengths within the $K=0-$ ground-state rotational band.

I_i	$M1$ transition (keV)	$E2$ line (keV)	C^2/q^2
3	116.8	88.6	∼0.32[a]
5	149.9	158.7	0.42±0.10
7	179.8	227.8	>0.27±0.08
6	48.0	197.3	0.29±0.07

[a] Error greater than 30%.

B. The $K=3+[523\uparrow-521\downarrow]$ Band

The strongest γ transition in the low-energy spectrum, the 136.6-keV $E1$ transition, can, because of its high-intensity feed either the 54-keV state or the 171-keV level. Estulin[23] has not observed coincidences between the 136 and 116 keV lines, in spite of the fact that the 116-keV line is a fast $M1$ transition according to our interpretation. Therefore, the 136-keV line originates from a state at 190.901 keV in accordance with Estulin's assumption. The isomeric level at 190 keV decays in fact by means of two $E1$ transitions to the 2− and 3− states[20] and has spin parity 3+ because no transition to the 1− state has been observed. The 190.9-keV level (see Sec. IIIA) is also excited directly from the compound state by a strong high-energy (n,γ) transition which therefore probably is an $E1$ transition.

Other intense high-energy lines populate states at 263.2±1 and 372.5±0.5 keV (see Table II). These

[59] B. R. Mottelson (private communication).
[60] Å. Bohr and B. R. Mottelson, At. Energ. (USSR) 14, 41 (1963).

transitions are probably also $E1$ which would imply positive parity for these states. General population considerations[58] require that the transitions de-exciting these levels are relatively strong. Considering the available transitions from Table III and their intensities along with the intensity of 0.3% for the primary transition into the 372.5-keV level, it is found that this state must decay through the 181.086-keV transition to the 190.901 keV 3+ level. This results in an energy of 371.984 keV for the 372-keV state. The combination principle applied to intense transitions (see Table IX, line 6 and Appendix A) yields then a level at 260.661 keV which decays through the 69.76-keV line leading to the 190.901-keV level. The multipolarity of this transition has been measured in this experiment to be mostly $M1$ implying positive parity for the 260.661-keV state. The value 260.661 keV differs appreciably from the energy which is found from the high-energy data. This indicates that the 263.2±1.0-keV level suggested from the high-energy capture data is probably a complex state. This will be discussed later in Sec. H.

The strong 87.595-keV $M1$ transition and the moderately strong 157.344-keV transition combine with the 69.760-keV transition to yield a level at 348.257 keV with positive parity. An additional state is obtained through the 193.107-keV line and the 105.517-keV $M1$ transition which form a closed loop with the 87.595-keV line. This level at 453.77 keV must also have positive parity.

Two additional transitions, the 89.599- and the 262.93-keV lines out of the many lines given in Table III can be fitted between the states which we have found so far. A simple statistical calculation gives 1.5 as the number of accidental fits if we consider all transitions from Table III. The transitions which we have used before (except for the 227.8-keV line) are strong in the sense defined in Appendix A. The probability that they combine by accident is small. This is no longer the case if we consider transitions as weak as the 89.599-keV line (which might connect the 260.66-keV level and the 3− state at 171.0 keV) and the 262.93-keV transition (which might connect the 453.77 keV and 190.90-keV states). Perhaps these two transitions fit by accident. In fact, we believe that the 89.599-keV line does fit by accident because of the absence of other transitions to the 1−, 2−, and 4− levels of the ground-state band.

The 453-, 348-, and 260-keV levels apparently do not decay to any member of the $K=0-$ band. These states and the 190-keV level not only have the same parity, they are also connected through intense stopover $M1$ lines and weaker crossover transitions. This strongly indicates that the four levels have similar structure. Therefore, the 262.93-keV line is expected to be much stronger than the 105.5- or the 193.1-keV transitions, if it corresponds to a transition from the 453-keV state to the 190-keV level. In contradiction to this, the 262-keV line is very weak. We therefore believe this fit to be accidental. The absence of a strong line from the 453-keV level to the 190-keV state implies that their spins differ by more than 2. The only reasonable spin assignments for the 260-, 348-, and 453-keV levels are 4+, 5+, and 6+, respectively.

The similarity of these states with a $K=3+$ rotational band is evident. The application of the rotational energy formula with the energies of the 3+, 4+, and 5+ levels yields

$$A=8.6500 \text{ keV}\pm0.5 \text{ eV}$$

and

$$B=+2.19 \text{ eV}\pm0.02 \text{ eV}.$$

The calculated energy for the $6+ \rightarrow 5+$ transition is 105.692 keV±25 eV, rather close to the observed value. A value of $E_{\text{calc}}=124.135\pm0.040$ keV is computed for the $7+ \rightarrow 6+$ transition energy. We find a loop using the 123.437 keV±10-eV line and the 229.00±0.07-keV transition, indicating the 7+ state at 577.21 keV. The 7+ state cannot be based on the combination principle alone because of accidental combinations. However, the combination together with the total population of the proposed 7+ level as compared with the prediction from general population considerations and the fact that both the energy of the 7+ state and the branching ratio of the transitions depopulating this level fit well into the systematics expected within a rotational band strongly indicate that the 7+ state is at 577.21 keV.

It is clear that the proposals of the 7+ and 7− levels are partially based on the prediction of the rotational model. For this reason, these levels and the corresponding transitions have been dashed in the level scheme (Fig. 7).

Table V shows that, in analogy to the situation in the $K=0-$ band, the transition strengths are fairly constant within the $K=3+$ band. In calculating the ratios C^2/q^2, we have allowed for $E2$ components in the $I \rightarrow I-1$ transitions. Assuming a quadrupole moment of 8 b, we find $C^2 \approx 3.5$, a value which is much smaller than that in the $K=0-$ band.

Our results confirm the level energies and $I\pi K$ assignments from the $Ho^{165}(d,p)$ reaction.[17] The configuration $[523\uparrow-521\downarrow]$ seems most reasonable for the $K=3+$ band, in particular, since then an $E1$-transition to the $[523\uparrow-633\uparrow]$ levels of the ground-state band is intrinsically forbidden. The long partial half-life of the 136.6-keV transition (about 0.4 msec)[20] cannot be explained on the basis of normal K forbiddenness assuming an average hindrance factor of 100 per degree of

TABLE V. γ transition strengths within the $K=3+$ band.

I_i	$M1$ transition (keV)	$E2$ line (keV)	C^2/q^2
5	87.6	157.3	0.071±0.024
6	105.5	193.1	0.081±0.012
7	123.4	229.0	~0.10[a]

[a] Error greater than 30%.

forbiddenness. One has to assume admixtures of other configurations into the $K=0-$ or $K=3+$ band or both to allow an $E1$ transition. The assumption that the amplitude(s) of the admixed configuration(s) are rather small may well explain the long lifetime of the isomer at 190.9 keV.

C. The $K=4+[523\uparrow+521\downarrow]$ Band

In addition to the primary (n,γ) line populating the level at 371.984 keV mentioned in Sec. B, another high-energy γ-ray transition excites a level at (471.8±0.8) keV. The measured multipolarity of both the 111- and 181-keV transitions depopulating the 371.98-keV state to 3+ and 4+ states at 190.9 and 260.66 keV implies positive parity [as also indicated from the high-energy (n,γ) data], and spin 3 or 4 for the 372-keV level.

An energy of 470.839 keV is found for the 471-keV state using energy combinations involving the positive-parity states and the 122.577-keV and 98.857-keV $M1$ transitions. The parity of the 471-keV level is consequently positive, in line with the indication from the strength of the high-energy population. The strong 98.8-keV $M1$ transition to the 371-keV state implies that this level and the 470-keV state belong to the same configuration. The absence of a strong transition from the 470-keV state to the 190-keV level and the presence of a transition to the 348-keV $I=5+$ state require the spin of the 470.8-keV level to be 5+. Thus, the spin parity of the 371.9-keV level is 4+. A weak 279.8-keV line fits within 1.4 times the statistical error between the 470.8- and 190.9-keV states; if this tentative assignment is correct, then the multipolarity of the 279-keV transition is $E2$, consistent with its weak intensity.

The extremely weak 299.9-keV line which, because of its energy, would fit between the 470.8-keV level and the 171-keV 3− state cannot be identified with this transition because its multipolarity would be $M2$. Then a much stronger $E1$ transition to the 4− state at 181 keV should be seen, which is clearly absent.

Three transitions with energies of 117.2, 216.1, and 134.3 keV strongly indicate the existence of a level at 588.10 keV which should then have spin and parity 6+ because of its decay modes.

The three states at 371, 470, and 588 keV resemble a $K=4+$ rotational band. Comparing the observed energy spacing with what is to be expected according to the rotational formula, we obtain

$$A=10.1441 \text{ keV}\pm 1.5 \text{ eV},$$
$$B=-5.17 \text{ eV}\pm 0.03 \text{ eV}.$$

This band very probably has the intrinsic Nilsson structure $[523\uparrow+521\downarrow]$. One would expect that the $K=3+$ and $K=4+$ bands strongly couple with each other. Both the interband transitions and especially the fact that the branching ratio of the 111- and 181-keV transitions does not obey Alaga's rules[61] are indicative of this mixing. Perhaps an equally strong argument for mixing is the difference in the moments of inertia. In second-order perturbation theory one would expect that

$$\left(\frac{\hbar^2}{2\Im}\right)_4 \geq \left(\frac{\hbar^2}{2\Im}\right)_3$$

if the states are mixed. This is in agreement with the observations. We find also that the triplet state has the lower excitation energy in agreement with the Gallagher-Moszkowski coupling rules.

D. The $K=7-[523\uparrow+633\uparrow]$ Band

The total population of the long-lived 7− state in Ho^{166}, as determined in the present experiment, corresponds to a partial cross section of 3.5 b which is consistent with the partial cross section[62] for the population of the 0− ground state. Therefore, one expects that a few low-energy γ transitions feeding the 7− state should be among those given in Table III. General population considerations indicate that the excitation of the 8− state expected within the frame of the rotational model should be strong enough for the $8-\rightarrow 7-$ transition to be seen in Table III. The 136±2-keV (d,p) state which has not been assigned by Struble *et al.*[17] and the 5±2-keV (d,p) level obtained during our re-evaluation of all (d,p) data differ by 131±3 keV. Several low-energy γ rays have energies which are consistent with this value. Most likely the 131.759-keV line corresponds to the transition between these two levels, which are very probably the $I=7-$ and 8− levels of the $K=7-[523\uparrow+633\uparrow]$ band. Our tentative assignment is in even better agreement with the theoretical relative (d,p) cross sections as calculated by Struble than the previous assignment by Struble *et al.*,[17] where the 8− level has been proposed at 151 keV. The rotational parameter $\hbar^2/2\Im$ for this band would thus be 8.2350 keV which is about 8% smaller than the value of the $K=0-$ band. The $I=9-$, $K=7-$ level should then lie at about 284 keV which is appreciably smaller than the energy (308 keV) proposed previously.[17] The (d,p) data do not contradict the 284-keV value since the weak proton group which is then expected is too close to the intense line which comes from the (d,p) excitation of a 294-keV state. On the other hand, the supposed 308-keV state may be the low-energy tail of the intense "294-keV" group, so the (d,p) data do not unambiguously require the existence of a 308-keV level.

It is evident that our data only indicate the 7− and 8− levels of the $[523\uparrow+633\uparrow]$ band, our information coming almost exclusively from the (d,p) results and a comparison with a theoretical model.[17] For this reason,

[61] G. Alaga, K. Alder, Å. Bohr, and B. R. Mottelson, Kgl. Danske Videnskab. Selskab, Mat. Fys. Medd. **29**, No. 9 (1955).
[62] L. Seren, H. N. Friedlander, and S. Turkel, Phys. Rev. **72**, 888 (1947).

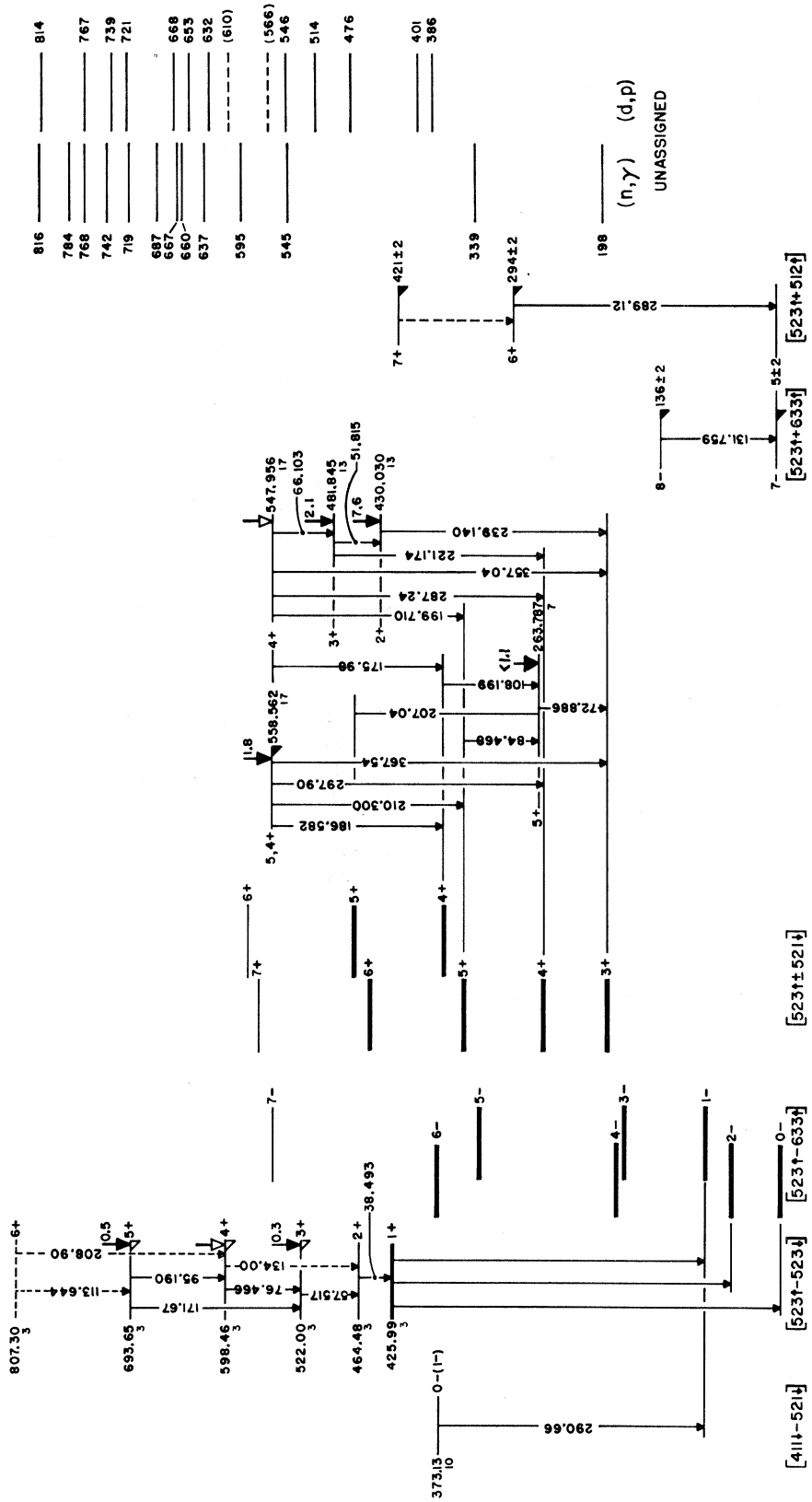

FIG. 8. Tentative extension of the firm part (Fig. 7) of the Ho^{166} level scheme. The level energies and the errors are absolute (keV). Unassigned levels from both the (d,p) and high-energy (n,γ) reactions are shown on the right. All levels from Fig. 7 are shown, in general, without the transitions. Bold levels are those believed most certain. See Fig. 7 caption for symbol conventions.

TABLE VI. Energies (in keV) and intensities of γ transitions from the β decay of Dy^{166}.

	Helmer[a]	Geiger[b]	Gunnink[c]	Brabec[d]	This experiment	I^e $K_i=1$	I^f $K_i=0$
E_1	428±2	440±10	427	425.8±0.4	425.99±0.03		
E_2	375±2	385±10	371	371.6±0.4	371.75±0.03		
E_3	344±2	···	343	343.0±0.6	343.51±0.03		
E_4	288±4	···	···	···	290.66±0.10		
I_1	1.4±0.1	1.36	1.31	1.30±0.10	1.36±0.20	1.36	1.21
I_2	1.1±0.1	1.14	1.16	1.17±0.10	1.10±0.16	0.36	1.26
I_3	$0.3\pm_{0.2}^{0.1}$	···	0.08	0.12±0.03	0.14±0.03	1.37	0
I_4	$0.10\pm_{0.08}^{0.05}$	···	···	<0.036	0.031±0.005		

[a] See Ref. 1.
[b] See Ref. 2.
[c] See Ref. 4.
[d] See Ref. 5.
[e] Theoretical relative intensities assuming initial K value of 1.
[f] Theoretical relative intensities assuming initial K value of 0.

we include these states only in our tentative level scheme (Fig. 8).

E. The $K=6+[523\uparrow+512\uparrow]$ Band

The lowest two levels of this band have been proposed in the work by Struble *et al.*[17] to be at 294±2 keV ($I=6+$ state) and 421±2 keV ($I=7+$ level). The population of the 6+ state is estimated to be of the order of a few percent in the (n,γ) reaction. Its decay should occur to the $7-[523\uparrow+633\uparrow]$ level only via a 289±3-keV $E1$ transition. Indeed, a 289.120-keV $E1$ transition with reasonable intensity is found in the low-energy (n,γ) spectrum. This line strongly supports the assignments of the 7− and 6+ states. Another line close in the energy, the 287.2-keV transition, seems too weak. The (d,p) data predict a 127±3-keV line as the $7+\rightarrow 6+$ transition within the $K=6+$ band. The 124.35-, the 128.56-, and 129.35-keV γ transitions can be considered as candidates. Again, the small amount of information about these levels coming mostly from (d,p) data suggests that the assignment of these states be considered tentative (see Fig. 8).

F. Levels Populated through the Dy^{166} Decay

1. The 373-keV Level

Except for the γ-ray transitions depopulating the 425.99-keV level shown in Fig. 7, and the 290.660 ±0.100-keV line, no further γ transitions have been found during the β decay of Dy^{166}. In agreement with the coincidence data of Helmer,[1] we assume that the 290.66±0.10-keV transition depopulates a level at 373 keV. This transition should then be fairly intense in the $Ho^{165}(n,\gamma)Ho^{166}$ spectrum. In fact, the 290.61±0.03-keV $M1$ transition agrees nicely in energy with the decay line and has a proper intensity. If these two transitions are identical, then the level at 373.08±0.03 keV has negative parity. Assuming in the Dy^{166} decay that the 373-keV state is fed only through a beta branch, we obtain a logft value of about 7.6 for this β group. This independently supports the negative parity assignment of the 373-keV level and requires spin 0− or 1−, a unique first-forbidden transition being considered less probable. The depopulation of the 373 level to only the 1− state favors spin 0−. However, the spin 1− assignment cannot be completely excluded. On the basis of energy considerations only, the most probable configuration for either spin assignment is either the parallel or antiparallel coupling of the $[411\downarrow]$ proton orbital and the $[521\downarrow]$ neutron orbital, that is $[411\downarrow\pm 521\downarrow]$.

2. The 426-keV Level

This state which has been observed in the Dy^{166} decay experiments is independently obtained from the low-energy (n,γ) data through energy combinations using strong transitions (see Table IX). The comparison of the data found in this experiment with the results from decay studies (see Table VI) clearly shows that our 425.99-keV state is identical with the 425-keV 1+ level which is excited through an *au* β branch with a logft value of about 4.88 requiring the configuration $[523\uparrow-523\downarrow]$.[63] The branching ratio of the transitions from this state to the 0−, 1−, and 2− levels of the ground-state band is not in agreement with Alaga's rules, assuming unmixed states. A possible explanation of this dilemma is[64] that differences in the small amplitudes of admixed states may account for the deviations from Alaga's rules, since $E1$ transitions usually are strongly hindered. In the case of an intrinsic $[523\downarrow]\rightarrow[633\uparrow]$ transition the selection rules[34] do not allow an $E1$ transition within the single-particle model. This transition has not been observed[65] in Dy^{165}, thus indicating a strong hindrance.

[63] We are very much indebted to Dr. M. E. Bunker for discussion of this point.
[64] We are very grateful to Professor P. Gregers Hansen who drew our attention to this point.
[65] O. W. B. Schult, B. P. Maier, and U. Gruber, Z. Physik 182, 171 (1964).

G. The $K=1+[523\uparrow-523\downarrow]$ Band

The level scheme obtained so far: the $K=0-$, $3+$, and $4+$ bands and the 373.0- and 425.9-keV states comprise together 18 levels. Most of the transitions which are strong in the sense explained in the Appendix A, so that they can safely be used in energy combinations, have been assigned. There is no conclusive evidence for the existence of combinations including several of the remaining "strong" lines. On the other hand, the chance that a transition fits by accident between an arbitrarily assumed new state and the 18 levels is of order 1 when all of the remaining γ lines are used for combinations. Under this set of circumstances it is difficult to prove the existence of additional states. Instead, we assume that a rotational band will be built on the $1+[523\uparrow-523\downarrow]$ band head at 425 keV and proceed by checking whether our data are consistent with the expected rotational structure.

Assuming a rotational parameter $A=\hbar^2/2\Im\approx 9$ keV for this band, we expect the $2+$ state roughly 36 keV above the $1+$ level. The 38.4-keV $M1$ transition (Table III) has the right multipolarity, is sufficiently close to the expected energy and has a reasonable intensity. The $2+$ level is therefore probably at 464.480 keV. Assuming the "rotation-vibration parameter" B is zero, an energy of about 57.7 keV is expected for the $3+\rightarrow 2+$ transition. We tentatively assign the 57.517-keV line to this transition and obtain 521.99 keV as a probable energy for the $3+$ state. The $3+$ to $1+$ crossover transition is expected to be too weak to be observed in the low-energy γ-ray spectrum because of a relatively intense nearby line. Continuing the development of the rotational band using the combination principle which, as mentioned previously, must be satisfied within the statistical errors, we find tentatively 598.46 keV for the $4+$ level, 693.65 keV for the $5+$ states and possibly 807.29 keV for the $6+$ member of the $K=1+[523\uparrow-523\downarrow]$ band.

From the transitions between the $3+$, $2+$, and $1+$ levels we derive

$$A=9.6530\text{ keV}\pm 2.2\text{ eV}$$

and

$$B=-3.7\pm 0.2\text{ eV}.$$

The small value of the B parameter supports the existence of the $1+$ band as well as the moment of inertia which is found to be 7% smaller than in the ground-state band. A comparison of the branching ratio of the transitions within this band shows that the $M1$ transitions are very fast and yields values for C^2/q^2 which are reasonably constant (see Table VII). This and the observation of two, possibly three, high-energy (n,γ) lines, the energies of which are consistent with the assumption that they populate the $3+$, $4+$, and $5+$ members of the $K=1+$ band, additionally support the $1+$ band. Several γ lines fit between the $K=1+$ levels and states of the $K=0-$ ground-state band. However, the observed branching ratios cannot be understood in terms of Alaga's rule. In view of the lack of a theoretical model explaining interband γ branching ratios particularly for $E1$ transitions in odd-odd deformed nuclei, we do not know whether these energy fits are real or accidental.

TABLE VII. γ transition strengths within the $K=1+$ band.

I_i	$M1$ transition (keV)	$E2$ line (keV)	C^2/q^2
4	76.4	134.0	~ 0.5[a]
5	95.1	171.6	0.26±0.07
6	113.6	208.9	0.26±0.07

[a] Error greater than 30%.

Our evidence for the $K=1+$ band strongly rests on the rotational model. For this reason, these levels have only been included in our tentative scheme (see Fig. 8).

H. Further Levels

The strongest high-energy γ transition (probably $E1$) excites a level at 430.1±0.5 keV which should therefore have positive parity. The most likely mode of decay of this state is the intense (4.2%) 239.140-keV transition leading to the 190.9-keV $3+$ state, resulting in a $2+$, $3+$, or $4+$ level at 430.0 keV, an excitation energy which agrees with the high-energy (n,γ) value. The absence of further transitions to other states, the energies of which have been determined precisely, favors spin $2+$.

Returning to the complex level observed through the high-energy (n,γ) data at 263.2±1.0 keV, the low-energy capture spectrum may be used to see if a second state near 263 keV seems plausible. The energy of the sum of the 108.199- and 72.8859-keV transitions equals the energy of the 181.086-keV line well within the expected precision (see Table IX). This combination, assuming the 108.2-keV line depopulates the 371.984-keV state, yields a level at 263.787±0.007 keV. This might well account for the observed high-energy primary line; also two unresolved high-energy transitions to states at 260.661 and 263.787 may be present. The measured multipolarities of the 108.2-keV line and the 72.88-keV line indicate spin $5+$ for the 263.787 level which is probably excited via two more transitions: an 84.4-keV transition from the $5+$ level at 348.2 keV which fits into a well-closed energy loop (see Table X), and a 207.0-keV transition from the $5+$ state at 470.8 keV. These modes of excitation and de-excitation, including the primary high-energy transition, are then entirely consistent with the existence of a state of spin and parity $5+$ at 263.787 keV.

The de-excitation of the 430- and 263-keV levels is easily understood if we assume that the 430-keV state has the configuration $K=2+$ $[523\uparrow-521\uparrow]$ and that the 263-keV state is $K=5+[523\uparrow+521\uparrow]$. These configurations are theoretically predicted to be at higher excitation energies. Somewhat lower-lying excited proton configurations which also give $K=2+$ and $K=5+$

TABLE VIII. Comparison of level energies of Ho^{166}.

(n,γ) Low energy		(n,γ) High energy[a]		(d,p)[b]	
E (keV)	$I\pi K$	E (keV)	dE (keV)	E (keV)	$I\pi K$
0	0−0	...			
		...		5±2	7−7
54.239	2−0			53±2	2−0
82.470	1−0	...		82±3	1−0
				136±2	8−7
171.074	3−0	170.8	0.8	(168±2)	(3−0)
180.467	4−0			181±1	4−0
190.901	3+3	190.9[c]		191±1	3+3
		197.9	2		
260.661	4+3	263.2	1	260±2	4+3
263.787	(5+5)				
		...		294±2	6+6
		...		308±3	(9−7)
329.775	5−0	330.7	3	330±2	5−0
		338.8	2.5		
348.257	5+3			348±2	5+3
371.984	4+4	372.5	0.5	373±2	4+4
373.13	(0, 1−)	...			
377.806	6−0	...			
				(386±2)	
				(401±2)	
		...		421±2	7+6
425.990	1+1	...			
430.041	(2+2)	430.1	0.5		
453.772	6+3	...		457±2	6+3
464.480	2+1				
470.839	5+4	471.8	0.8	469±2	5+4
				476±1	
481.845	(3+2)	481.6	0.7		
				514±1	
521.996	3+1	522.1	2	524±2	
		544.7	1.5	546±2	
547.956	(4+2)				
557.688	(7−0)	...			
				557±2	
558.562	(5, 4+)	558.9	1		
				(566±2)	
577.210	(7+3)	...		(578±3)	
588.103	(6+4)	...		589±2	
		594.7	0.8		
598.462	4+1	602.3	2	599±2	
				(610±2)	
				632±1	
		637.3	1.2		
				653±1	
		659.7	1.5		
		666.6	2	668±2	
		686.6	2		
693.652	5+1	693.7	1.5	691±1	
		719.1	0.7	721±2	
		741.8	2.5	739±1	
		767.8	4	767±1	
		783.7	3		
(807.296)	(6+1)	...			
		816.2	0.5	814±1	
		829.8	1		
		881.6	1		
		890.6	1	891±1	
		905.2	1	907±3	
				925±2	
				(942±3)	
		961.6	3	961±1	
				982±1	
		1006.0	1.5	1007±1	
		1030.3	0.7		
				1035±1	
				1057±1	
		1062.1	0.7		
				1080±2	
		1089.3	1.5		
		1099.3	2		
				1105±1	
		1117.9	2	1122±2	
		1137.0	1.5	1137±2	
				1154±3	
		1160.4	1.5		
				1173±1	
		1191.7	1	1188±1	
		1204.0	2	(1205±2)	
		1216.0	2		
				(1221±2)	
		1231.6	0.8		
				(1245±2)	

[a] Three dots for the high-energy (n,γ) entry indicates that quadrupole or higher multipole would be expected from the assigned spins.
[b] Alignment of (d,p) and (n,γ) states in those cases where a spin assignment has not been made from the (d,p) cross section suggests only energy agreement. The excited states may not be identical.
[c] Reference line used to establish the excitation energy scale.

bands are [411↑±633↑]. The structure of the $K=2+$ and $K=5+$ bands may be an admixture of these configurations. That component of the wave function of these bands resulting from the excited proton configurations would give rise to $M2$ transitions to the ground state which would not compete strongly with the decay of the configurations [523↑±521↑] to the $K=3+$ and 4+ bands. These configurational assignments are consistent with the absence of excitation of these levels in the (d,p) process. The relative energy of the $K=2+$ and 5+ bands is in agreement with the Gallagher-Moszkowski coupling rules and the feeding of the 263.7-keV level can be understood in terms of mixing of the neutron configuration [521↑] and [521↓].

Another intense high-energy line populates a level at 481.6±0.7 keV, the parity of which should be positive and the total population of which is expected to be a few percent using general population considerations. Assuming that a rotational band is built upon the $K=2+$ state at 430 keV, one would expect from the model a 3+ state some 50 to 60 keV above the 430-keV state. If the 481.6-keV state corresponds to the expected 3+ level, the 3+ to 2+ transition should have an energy of approximately 51.6 keV. The observed transition of 51.8155 keV is reasonably intense and can be identified with this expected transition. The 3+ level at 481.6 keV would also be depopulated through the strong 221.174-keV line, the multipolarity of which implies positive parity for the level, which then becomes 481.845 keV. The parity is consistent with the assumption that this state is the 3+ member of the 2+ rotational band. According to the rotational energy formula,

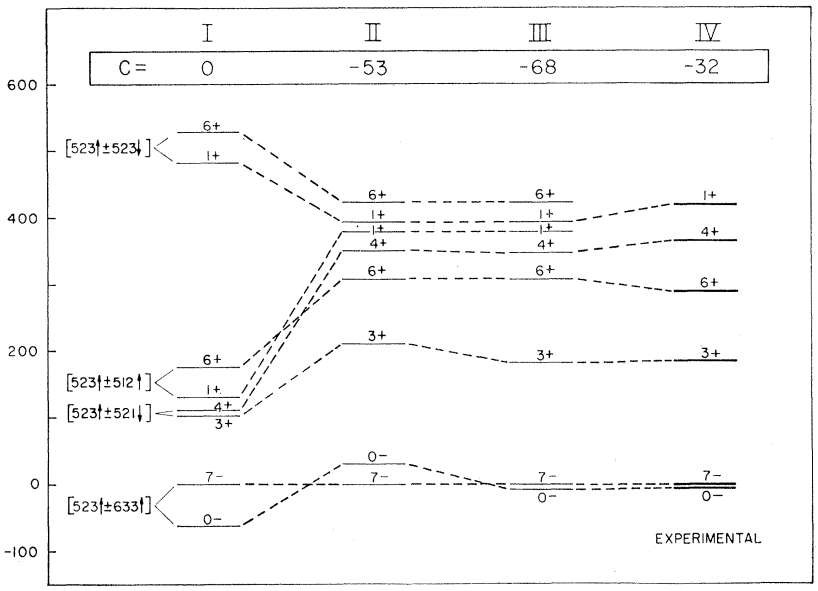

FIG. 9. Comparison of the experimentally observed states and the theoretically predicted energies. Column 1 gives the predictions for the zeroth-order model. Column 2 displays the results when the first-order effects of H_{INT} are included. Column 3 shows the results when configuration interactions and the Coriolis effects are taken into account. The quantity C is one-half of the energy shift between the even and odd members of the $K=0$ rotational band.

one would predict the expected 4+ member of this band to lie about 69 keV above the 3+ state. Assuming that the observed transition of 66.103 keV connects the 4+ and 3+ states, one finds numerically that the intense 199.710-keV transition observed can depopulate the 4+ state to the 5+ state at 348.257 keV. Additional transitions probably connect the 4+ state at 547.956 keV with the 4+ state at 371.984 keV (175.98-keV line), the 3+ state at 190.9 keV (357.04-keV line) and to the 4+ state at 260.6 keV (287.24-keV line). From these energies for the 2+, 3+, and 4+ members, one finds for the $K=2+$ band:

$$A=9.1138 \text{ keV},$$
$$B=-26.55 \text{ eV}.$$

This is a very large value for B and is probably due to mixing of this band with other bands. The strong $M1$ transitions from the levels I_i of this $K=2+$ band to states $I_f=I_i+1$ belonging to the $K=3+$ band are probably the result of the neutron spin-flip associated with the neutron orbitals [521↑] and [521↓].

Another strong high-energy transition which is probably $E1$ defines a level at 558.9±1 keV which may also be found through the following combinations:

186.582-keV ($M1$,$E2$)
transition to the 4+ level at 371.98 keV;
210.300-keV ($M1$)
transition to the 5+ level at 348.26 keV;
297.90-keV ($M1$)
transition to the 4+ level at 260.66 keV;
and
367.54-keV transition to the 3+ level at 190.90 keV.

The first two transitions yield an energy of 558.562 keV±17 eV for the state in question. The combination is strongly supported by the multipolarities of the transitions and implies spin parity 5+ or 4+ for the 558-keV state in good agreement with the high-energy data.

Further effort to assign low-energy lines to transitions depopulating levels which have been seen either in the high-energy (n,γ) work or through the (d,p) reaction is difficult because of the large number of accidental combinations. For this reason, our experimental data, which in fact contain much more information than we could incorporate in the decay scheme (Fig. 7) or its tentative extension (Fig. 8), should be combined with other experiments which we shall propose in the conclusion of this work. The numerical results obtained from the different experiments including the (d,p) data[17] are compared in Table VIII.

V. COMPARISON OF THE THEORETICALLY PREDICTED AND THE EXPERIMENTALLY OBSERVED LEVEL SPECTRUM

The purpose of this section is to discuss the quantitative effects of H_{INT} and so to sensitively test the model which has been indicated briefly in Sec. II. The details of the formalism are given in Appendix B. We do not fit the levels characterized with maximum precision, but rather only with a minimum number of parameters in order to understand the effect of H_{INT}. In particular, we give here the results of the calculations involving the band head positions and the splitting within $K=0$ bands, and compare these with the experiment, the calculation being only qualitatively described.

The single-particle energies for the proton and neutron were taken from the available experimental information on Ho^{165} and Dy^{165} (see Table I). After the rotational contribution to these energies was removed,

it was assumed that these energies were the eigenvalues of H_p and H_n. The entire energy matrix for each spin and parity value of interest was formed and diagonalized in a set of basic vectors which were the eigenvectors of $H_R+H_p+H_n$. The form of H_{INT} was taken to be central and thus contained five parameters, the strengths for the singlet-even, singlet-odd, triplet-even, triplet-odd components, and a range. The radial dependence was chosen to be Gaussian. Altogether about fifty force mixes were tried but only a rather long-ranged force with little space exchange character gave an adequate fit to the experimental data. A final parameter was the inertial parameter ($\hbar^2/2\Im$) which was not free, but was chosen to be 9 keV, a value close to that for the ground-state rotational band. This parameter determines the strength of the Coriolis interactions.

In Fig. 9, a comparison between states of the calculated and experimental spectrum is shown and the details of the force are given in Appendix B. The general agreement between calculated order and observed intrinsic states in Ho^{166} is satisfactory. The calculated order and even the excitation energies agree well with experiment. It is particularly important to note that first-order effects of H_{INT} and H_{PP} cannot reproduce the observed spectrum, in particular with respect to the relative ordering of the doublet which comes primarily from the configuration $[523\uparrow\pm633\uparrow]$, $K=0-$, $7-$. Only strong configuration mixing due to the neutron-proton force can cause this violation of the Gallagher-Moszkowski rules. This implies very impure wave functions with the result that corrections must be made to the transition probabilities.

One expects, therefore, deviations from Alaga's rules in cases where interband transitions are considered, as for instance the transitions from the $1+$ state at 425 keV to levels of the ground-state band, or the transitions from the $K=4+$ band to the $K=3+$ band. As long as the collective nature of the levels is preserved, intraband transitions should not be affected too much. This is reflected in the experimental observation that the ratios C^2/q^2 as given in Tables IV, V, and VII are fairly constant.

Although in the case of odd-A nuclei, the neglect of the H_{RPC} term was, in general, not serious except for $K=\frac{1}{2}$ bands and even the asymptotic selection rules tabulated in Mottelson and Nilsson[34] were often very good, this cannot be assumed for odd-odd nuclei. The strong effects of the neutron-proton interaction in Ho^{166} severely compromises the purity of the wave functions, distorts the energy systematics of the zeroth-order model, and even causes a violation of the Gallagher-Moszkowski coupling rules in the ground state. Thus, unfortunately, it seems that extensive numerical calculations are necessary in order to give a reasonably complete description of the deformed odd-odd system. However, this should not be unexpected since this occurs in spherical odd-odd nuclei. What is interesting, and hopefully not unique to Ho^{166}, is that simple assumptions about the nuclear structure can lead to good quantitative agreement with experiment.

VI. THE ROTATIONAL MOTION

Very precise values have been obtained in this experiment for the excitation energies of the different members of rotational bands. It is interesting to compare the observed level spacings with those predicted from the simplest rotational energy formula:

$$E_I=E_0+AI(I+1). \tag{7}$$

Using this relation, one may extract the parameter A from the observed level spacing. Under these conditions, A is not a constant, but depends on I since the experimentally determined level energies cannot be described exactly by the above formula. We obtain the following relations:

$$\text{for } K=0: \quad A_I=\frac{E(I\rightarrow I-2)}{4I-2}, \tag{8a}$$

$$\text{and for } K\neq 0: \quad A_I=\frac{E(I\rightarrow I-1)}{2I}. \tag{8b}$$

The ratios $(A_{I+2})/A_I$ and $(A_{I+1})/A_I$ would be 1.00 in the case where Eqs. (8a) and (8b) are exactly satisfied. A plot of this ratio versus I indicates to what accuracy the rotation follows the above formula.

Plots of this type have been used by Stephens *et al.*,[66] who consider the phenomenological effect of stretching as contained in the Davydov-Chaban treatment[67] to be the reason for the deviation of the observed levels from the energy values expected from the simple rotational formula. Stephens *et al.*[66] excited levels with spins up to $I=18$ in the ground-state rotational bands of neutron deficient deformed even-even nuclei and found that the Davydov-Chaban theory does in fact permit an excellent fit to their data.

In studying (n,γ) radiation from Er^{168}, Koch[68] found the ground-state band with rotational members up to $I=8$, the γ band up to $I=8$, and two quasiparticle bands with levels up to $I=8$ and $I=7$. As can be seen from Fig. 10, Er^{168} is the most perfect rotor of the even-even nuclei studied so far. The ratios $(A_{I+1})/A_I$ for $I=4$ and 5 of the $K=3+[633\uparrow-521\downarrow]$ two-quasiparticle neutron band in Er^{168} clearly show that the exclusive assumption of a phenomenologically stretching nucleus is inadequate in this case. The same is true for the $K=3+$ band in Ho^{166} (see Fig. 10). We believe that several effects act together in affecting the excitation energies of rotational states in deformed nuclei: the stretching, i.e., the β-vibration-rotation interaction, the

[66] F. S. Stephens, N. L. Lark, and R. M. Diamond, Nucl. Phys. **63**, 82 (1965).
[67] A. S. Davydov and A. A. Chaban, Nucl. Phys. **20**, 499 (1960).
[68] H. R. Koch, Z. Physik **192**, 142 (1966).

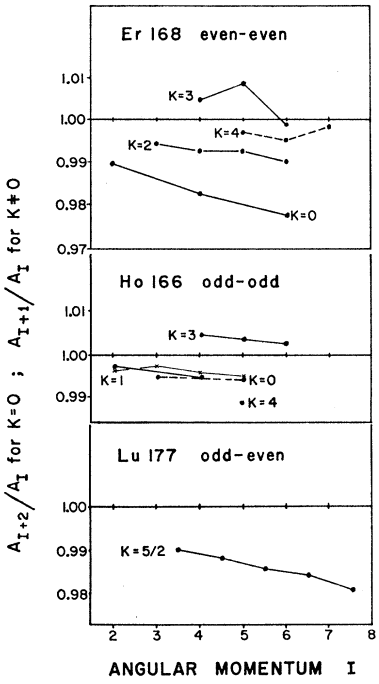

FIG. 10. Dependence of the experimental moment-of-inertia parameter on the spin I of the rotational levels. $A_I = E(I \to I-2)/(4I-2)$ for $K=0$ and $A_I = E(I \to I-1)/2I$ for $K \neq 0$.

γ-vibration-rotation interaction (as becomes evident from the necessity of the application of the z correction[69] in order to better explain the branching ratios of the transitions from the γ band to the ground-state band), the Coriolis antipairing (CAP) effect,[70] and other band-mixing effects. Figure 10 also shows the ratio $(A_{I+1})/A_I$ for one of the rotational bands in Lu^{177} which has been studied by Maier.[71]

The absolute values of the moments of inertia of all Ho^{166} bands shown in Fig. 8 fluctuate around the value $\hbar^2/2\Im \approx 9$ keV. Deviations from this average value are similar to those observed[65] for the [633↑], [521↓], and [512↑] bands in Dy^{165}. The B parameters of the $K=0-$, $3+$, $4+$, and $1+$ bands in Ho^{166} are much smaller than would have been expected if one compares with an even-even nucleus.

It has generally been assumed that the existence of a gap in an even-even nucleus should allow the highly collective states below the gap the opportunity for more exact rotational energy systematics particularly because of the greatly lessened Coriolis coupling. The comparisons presented in Fig. 8 seem to refute this assumption at least in Ho^{166}.

VII. CONCLUSIONS

The investigation of the nuclear level scheme of Ho^{166} as presented in this work has revealed several well-developed rotational bands. The Nilsson model in its two-quasiparticle version seems to successfully interpret this odd-odd deformed nucleus. Both configurations corresponding to the $K=\Omega_p+\Omega_n$ and $K=|\Omega_p-\Omega_n|$ coupling of the odd proton and odd neutron are indicated for the [523↑] and [633↑], the [523↑] and [521↓], and the [523↑] and [521↑] Nilsson states. There is good evidence for the [523↑−523↓] band and the [523↑+512↑] band. Probably the [411↓−521↓] state has been observed at 373 keV. This is so far the only evidence for a proton-excited state in Ho^{166}.

Several levels are directly excited through high-energy (n,γ) transitions from the compound state. Data on the direct population of rotational bands in highly deformed nuclei are not available to the degree that fluctuations within a band or to various bands can be reasonably compared. Only the 3− and 5− levels of the ground-state band are fed from the compound state. No direct population of the 2− state has been observed. It is not clear whether one should conclude from this that only the 4− compound state is responsible for the direct excitation of levels in the ground-state band. Apparently a K-forbiddenness is no longer effective here. The lack of the direct transition to the 5+ member of the $K=3$ band is hard to understand on the basis of a statistical fluctuation. According to our interpretation the 3+, 4+, and 5+ states, being members of the same rotational band, should have similar wave functions.

Many details which have been proposed in our level scheme (Fig. 8) require further experiments:

The $K=7-$[523↑+633↑] band should be investigated utilizing the Coulomb excitation of Ho^{166} nuclei in the 7− state with a half-life of 1200 years. This half-life is sufficiently long to make the experiment easier than the Coulomb excitation[72] of Tm^{170}. The proposed experiment, although difficult, could serve to determine the $9- \to 8- \to 7-$ level spacing and possibly the position of vibrational states. This information could then be compared with our (d,p) level energies and, if obtained with sufficient accuracy, even the particular γ transition(s) could be utilized from Table III.

The decay of the 430- and 481-keV states should be studied in a coincidence experiment. In this particular case, very strong primary capture transitions are involved which increase the feasibility of this experiment. Considerable additional knowledge could be gained through a $(d,p\gamma)$ experiment. In view of the level density, however, this experiment will probably prove to be very difficult.

Finally it is hoped that in the future the experimental techniques used in this work can be improved so that data with still higher quality can be obtained.

ACKNOWLEDGMENTS

We wish to thank Professor H. Maier-Leibnitz, Professor O. Kofoed-Hansen, and Professor K. Sieg-

[69] P. Gregers Hansen, O. B. Nielsen, and R. K. Sheline, Nucl. Phys. **12**, 389 (1959).
[70] T. Udagawa and R. K. Sheline, Phys. Letters **15**, 172 (1965).
[71] B. P. K. Maier, Z. Physik **184**, 153 (1965).
[72] H. Ryde, G. D. Symons, and Z. Szymanski, Nucl. Phys. **80**, 241 (1966).

bahn for their interest in, and sponsorship of, part of this research. Discussions held with T. Udagawa, A. Kerman, J. Griffin, and M. E. Bunker were particularly helpful. This work involved the use of four reactors and a Van de Graaff accelerator and we are indebted to the many people at these facilities who so efficiently assisted in their operation as well as in the processing of the large amount of data. The hospitality of the Danish Atomic Energy Commission extended to five of the authors is especially acknowledged.

APPENDIX A: ENERGY-COINCIDENCE TECHNIQUE

With sufficiently high precision and completeness, a γ-ray set representing transitions between a set of energy levels can be used to determine the energy levels themselves. This level determination in its most elementary form results from the combination of sums and differences between pairs of observed lines to equal a third line and the interlocking of such combinations. This is the counterpart of the time-coincidence experiment between pairs of γ rays, but in this case no knowledge of actual time relationships is known. Accurate energy loops can, however, similarly show the sequential relationship between two such transitions with no knowledge of which is emitted initially. This energy coincidence treatment is similar to the Ritz combination principle used in optical spectroscopy. The applicability of this combination principle is not affected when all experimentally determined relative energies E, as given in Table III, Column 1, are multiplied by a constant factor as for instance, the calibration factor to convert the relative energies into absolute energies (in keV). For this reason, only the errors dE which are given in Column 2 of Table III determine the uncertainty of the combination. These experimental errors, dE in relative energy determination, finite resolution and background impose limitations to the precision and completeness of the γ-ray set. This greatly limits the practical application of this procedure.

Consider the combination of a γ ray of relative energy E_a with one of relative energy E_i where the errors are dE_a and dE_i. The probability that the sum E_a+E_i will, within the total error dE_1, equal a third γ-ray energy, E_j whose error is dE_j is given by

$$W=2\delta E/(E_{\max}-E_{\min}), \tag{A1}$$

where

$$\delta E=\sum_\nu dE_\nu$$

and

$$dE_\nu^2=dE_a^2+dE_i^2+dE_j^2,$$

and the minimum and maximum energy values apply to the range of energies over which the γ rays E_i and E_j are available. This probability can be viewed as the ratio of the energy interval occupied by the errors to the total energy interval and is equivalent to the ratio of the average error to the average spacing between lines. Consider the set of γ rays given in Table III containing some 350 γ lines from 38 to 734 keV. For the case of an accurately measured γ ray, E_a, we may neglect the error dE_a and if $dE_i \sim dE_j$, the numerator reduces to

$$2\delta E=2\sum_\nu dE_\nu=2\sqrt{2}\sum_j dE_j,$$

which is equal to 95 keV. The value of W is 0.14. For the case $E_a=69.76$ keV, some 300 values, E_i, must be considered. This corresponds to 0.14×300 or 42 random combinations. A computer search has found 35 such combinations for this γ ray and it is not possible generally to identify the combinations as being real rather than random.

This severe limitation to the consideration of energy loops for the entire set is due to the combination of the error magnitudes and the large numbers included in the set. Ideally, one would like to reduce the errors and retain the set, but with a given set, one can only endeavor to realistically restrict it somehow to extract the reliable combinations. The most important combinations to understanding the decay scheme are the ones involving the intense, accurately measured, transitions such as the 69.76-keV line. Consider the following combination:

$$E_a+E_i=181.0844 \text{ keV}=69.7604+111.324,$$
$$E_j=181.086,$$
$$dE=5.6 \text{ eV}=(1.4^2+2^2+5^2)^{1/2}.$$

Although this is an impressive combination, it is important to have some estimate of the random chance of its occurrence.

The resolution of the curved crystal spectrometer is high relative to line spacings for low-energy radiation. A low-energy "line" as listed will, therefore, rarely be composed of more than one transition, especially if the intensity is relatively high. The resolution is not as high at the higher energies, corresponding to 0.1%–0.4% at 400 keV. This means that a large fraction of the "lines" observed are probably unresolved multiplets. The observed energy of the "line" is then the centroid of the single components. The use of these measured values in energy loops then becomes very dubious both because of the multiplet possibility and because of the higher errors involved. It might seem reasonable, therefore, to confine the application of the combination or energy-coincidence principle to only the low-energy transitions. This, however, defeats the purpose most important to a development of the decay scheme which must of necessity include the most intense transitions even above 400 keV. It is important, however, to realize the experimental data will always lack information concerning weak crossover transitions in the higher energy range.

The ability of the spectrometer to detect weak lines

TABLE IX. Three-line combinations; the numbers E_1, E_2, E_3 are relative energies; dE_1, dE_2, dE_3 are their errors.

E_1	E_2	E_1+E_2	E_3	dE_1	dE_2	dE_3	dE	ΔE	$\Delta E/dE$
149.307	48.0315	197.3385	197.339	0.003	0.0007	0.008	0.009	0.0005	0.06
48.0315	179.882	227.9135	227.88	0.0007	0.004	0.07	0.07	0.033	0.5
69.7604	87.5946	157.355	157.344	0.0014	0.0016	0.008	0.008	0.011	1.3
87.5946	105.517	193.1116	193.107	0.0016	0.004	0.006	0.008	0.0046	0.6
105.517	123.437	228.954	229.00	0.004	0.005	0.07	0.07	0.046	0.7
69.7604	111.324	181.0844	181.086	0.0014	0.002	0.005	0.006	0.0016	0.3
72.8859	108.199	181.0849	181.086	0.0015	0.002	0.005	0.0056	0.0011	0.2
98.8570	117.264	216.121	216.160	0.0015	0.003	0.045	0.045	0.039	0.9
82.470	343.51	425.980	425.99	0.002	0.03	0.03	0.043	0.010	0.2
54.2392	371.75	425.9892	425.99	0.0007	0.03	0.03	0.043	0.0008	0.02

TABLE X. Four-line combinations.

E_1	E_2	E_3	E_4	dE_1	dE_2	dE_3	dE_4	dE	ΔE	$\Delta E/dE$
126.228	149.307	116.835	158.702	0.003	0.003	0.001	0.009	0.010	0.002	0.2
116.835	54.2392	82.470	88.60	0.001	0.007	0.002	0.03	0.03	0.004	0.14
87.5946	122.577	111.324	98.857	0.0016	0.004	0.002	0.0015	0.05	0.009	1.9
105.517	134.34	122.577	117.264	0.004	0.03	0.004	0.003	0.03	0.016	0.5
72.8859	84.468	69.7604	87.5946	0.0015	0.010	0.0014	0.0014	0.010	0.0011	0.11

as well as strong ones is a varying function over its energy range. The background at the higher energies certainly contains such weak, undetected transitions much more likely than in the low-energy region. The distinction between "strong" and "weak" lines is then an unknown function of the energy, the absolute value of which will depend upon the complexity of the particular spectrum under observation. Examination of Fig. 6, where the "lines" listed in Table III are plotted as points, gives an indication of the function representing the cutoff limit for observation of weak lines. It is the smooth curve formed by the lowest observed intensities. This imaginary curve will be called the "limit of constant intensity." Similar curves of constant strengths can be drawn by raising this lower limit curve on the log-log plot (Fig. 6). Points lying on such curves appear equally strong with respect to experimental conditions. Such curves are arbitrarily chosen as representing the best compromise for the selection of lines in order to arrive at an unbiased subset for estimating random errors of strong lines.

In the case of the example of 69.76+111.324 keV, there are only 15 unassigned lines "stronger" or as "strong" as the 111.324-keV line relative to a "curve of constant strength," covering an energy region from 108 to 543 keV. For this highly restricted subset, one finds $\sum dE=400$ eV which is far less than the value of about 34 keV for the entire set. The probability of a random combination W occurring in this smaller set is estimated from Eq. (A1) to be 0.6%.

The choice of a restricted set can, in such cases, clearly limit the possibility of random combinations and thus give confidence in the reliability of combinations of the type illustrated. Similar considerations must be applied to other cases in order that the chance of random combinations be restricted to a few percent. The levels given in Table VIII have been derived using only such highly reliable loops, after which other transitions of lower intensity and higher error can be fitted between levels. Further extrapolation of this technique to include a larger fraction of the spectrum requires both an increased precision and resolution and the corresponding lowering of the "limit of constant strength," at least for the higher-energy region.

Two examples may be given here showing to what degree of precision the combination principle is satisfied using, as has been explained before, our relative energy values E and the errors dE in the relative energy determination. Table IX contains triple combinations: $E_1+E_2\approx E_3$. Table X includes combinations involving four transitions each: $E_1+E_2\approx E_3+E_4$. ΔE is the discrepancy in the fit of the combination, dE is the error of the measurement. If all errors dE_i of the individual transitions E_i were purely statistical in nature, one would expect 68% of the ratios $\Delta E/dE$ to be less than one.

APPENDIX B: THEORETICAL MODEL FOR ODD-ODD DEFORMED NUCLEI

In describing an odd-odd nucleus, we consider that the unpaired proton and neutron move in a potential produced by a deformed core. The core is composed of pairs of protons and neutrons filling self-consistent single-particle states (approximated by Nilsson[9] orbitals) to a sharp Fermi surface. When the core experiences collective rotations, the total angular momentum is divided between the core and the valence particles. However, this description is oversimplified since, in addition to the correlations among the particles caused by the Pauli principle, an accurate description of the system must take into consideration the pairing correlations introduced by the short-ranged attractive part of

the $T=1$ two-body interaction which produces the stability of the core.

If, however, we take the single-particle energies for the valence particles from nuclei containing the odd system in question, in our case Ho^{165} and Dy^{165}, there will only be two sources of error in neglecting the pairing correlations. By deliberately assuming a sharp Fermi surface, certain off-diagonal matrix elements connecting particle- and hole-excited states vanish. When the pairing correlations are explicitly considered, there is a diffuse surface, and the matrix elements vanish only for highly excited states when the occupation probabilities tend to unity for the hole states. Similarly, most particle-particle off-diagonal matrix elements are overestimated. The second source of error occurs because of the blocking effect from the addition of a neutron (proton) to the odd-proton (-neutron) system. This causes the distribution of the pairs of neutrons (protons) to change among the self-consistent states. As a result they affect the self-consistent energies of the valence proton (neutron). These errors are difficult to estimate *a priori*. Therefore as the first step towards a fully microscopic description of deformed odd-odd nuclei we postulate the inert-core model.

We write the model Hamiltonian as

$$H=H_{\mathrm{R}}+E_p+E_n+H_{\mathrm{RPC}}+H_{\mathrm{PP}}+H_{\mathrm{INT}}, \quad \text{(B1)}$$

where

$$H_{\mathrm{R}}=\frac{1}{2\Im}[I^2-2I_3{}^2+2j_{p3}j_{n3}+j_p{}^2+j_n{}^2], \quad \text{(B2)}$$

$$H_{\mathrm{RPC}}=\frac{1}{2\Im}[I_+(j_{p-}+j_{n-})+I_-(j_{p+}+j_{n+})], \quad \text{(B3)}$$

$$H_{\mathrm{PP}}=\frac{1}{2\Im}[j_{p+}j_{n-}+j_{p-}n_{n+}]. \quad \text{(B4)}$$

Any set of basis vectors must be symmetrized in order to be invariant under rotations of $\pi/2$ radians about either the 1- or 2-body axis and under an arbitrary rotation about the 3-body axis. Thus a properly symmetrized particle-particle basis vector can be written

$$|IMK\alpha_i a_i\rangle=\frac{1}{\sqrt{2}}[\Phi^I{}_{MK}\xi_{\alpha_i}\xi_{a_i}+(-1)^{I+\pi+1}\Phi^I{}_{M-K}\xi_{-\alpha_i}\xi_{-a_i}] \quad \text{(B5)}$$

$$K=|\Omega_{\alpha_i}\pm\Omega_{a_i}|\,.$$

Here ξ_{α_i} is a Nilsson wave function labeled by α_i. A proton state is denoted by α_i and a neutron state by a_i. The parity of the basis state is denoted by $\pi(=\pm1)$. The Nilsson state conjugate to α_i (i.e., all quantum numbers are identical except $-\Omega_{\alpha_i}=\Omega_{-\alpha_i}$) is denoted by $-\alpha_i$. In this paper we use two different basis sets for the expansion of the Nilsson functions[73]

$$\xi_{\alpha_i}=\sum_{j,l} c^{\alpha_i}{}_{jl}R(p)_{n(\alpha_i)l}\chi(p)^{lj}{}_{\Omega(\alpha_i)}, \quad \text{(B6)}$$

which is a useful form for evaluating matrix elements of H_{R}, H_{RPC}, and H_{PP}, and

$$\xi_{\alpha_i}=\sum_{l,m} a^{\alpha_i}{}_{lm}R(p)_{n(\alpha_i)l}Y^l{}_m(\hat{p})\Sigma^{1/2}{}_{\Omega(\alpha_i)-m}(\hat{p}), \quad \text{(B7)}$$

which is a more useful form for evaluating matrix elements of H_{INT}. Using these bases, the matrix elements of H are given by

$$\langle IMK'\alpha_i a_i|H|IMK\alpha_j a_j\rangle=(\Phi^I{}_{MK'}\xi_{\alpha_i}\xi_{a_i},H\Phi^I{}_{MK}\xi_{\alpha_j}\xi_{a_j})+(-1)^{I+\pi+1}(\Phi^I{}_{MK'}\xi_{\alpha_i}\xi_{a_i},H\Phi^I{}_{M-K}\xi_{-\alpha_j}\xi_{-a_j}). \quad \text{(B8)}$$

In particular, if we consider H_{R}, then

$$\langle IMK'\alpha_i a_i|H_{\mathrm{R}}|IMK\alpha_j a_j\rangle=(\Phi^I{}_{MK'}\xi_{\alpha_i}\xi_{a_i},H_{\mathrm{R}}\Phi^I{}_{MK}\xi_{\alpha_j}\xi_{a_j})$$

$$=\frac{\hbar^2}{2\Im}\{[I(I+1)-2K^2+2\Omega_p\Omega_n]\delta_{i,j}+[\sum_{l,j} j(j+1)c^{\alpha_i}{}_{lj}c^{\alpha_i}{}_{lj}]\delta_{a_i,a_j}\delta_{\Omega(\alpha_i),\Omega(\alpha_j)}\delta_{N(\alpha_i),N(\alpha_j)}$$

$$+[\sum_{l,j} j(j+1)c^{a_i}{}_{lj}c^{a_i}{}_{lj}]\delta_{\alpha_i,\alpha_j}\delta_{\Omega(a_i),\Omega(a_j)}\delta_{N(a_i),N(a_j)}\}\delta_{K,K'}. \quad \text{(B9)}$$

H_{RPC} will have only nonvanishing nondiagonal matrix elements which are linear combinations of matrix elements given by

$$(\Phi^I{}_{MK'}\xi_{\alpha_i}\xi_{a_i},H_{\mathrm{RPC}}\Phi^I{}_{MK}\xi_{\alpha_j}\xi_{a_j})=-\frac{\hbar^2}{2\Im}[I(I+1)-K(K+1)]^{1/2}\{\sum_{j,l} c^{\alpha_i}{}_{jl}c^{\alpha_i}{}_{jl}[(j-\Omega_{\alpha_j})(j+\Omega_{\alpha_j}+1)]^{1/2}$$

$$\times\delta_{a_i,a_j}\delta_{\Omega(\alpha_i),\Omega(\alpha_j)+1}+\sum_{j,l} c^{a_i}{}_{jl}c^{a_i}{}_{jl}[(j-\Omega_{a_j})(j+\Omega_{a_j}+1)]^{1/2}\delta_{\alpha_i,a_j}\delta_{\Omega(a_i),\Omega(a_j)+1}\}\delta_{K',K+1}. \quad \text{(B10)}$$

H_{PP}, on the other hand, will have nonvanishing diagonal and nondiagonal matrix elements which are linear

[73] For typographical reasons, n_{a_i}, Ω_{a_i}, etc., will be printed as $n(a_i)$, $\Omega(a_i)$, etc., in some of the equations in this Appendix.

combinations of

$$(\Phi^I{}_{MK'}\xi_{\alpha_i}\xi_{a_i},H_{\rm PP}\Phi^I{}_{MK}\xi_{\alpha_j}\xi_{a_j})=\frac{\hbar^2}{2\Im}\{\sum_{\substack{j,l\\ j',l'}} c^{\alpha_i}{}_{jl}c^{\alpha_i}{}_{jl}c^{a_i}{}_{j'l'}c^{a_j}{}_{j'l'}$$

$$\times[(j\mp\Omega_{\alpha_j})(j\pm\Omega_{\alpha_j}+1)(j'\pm\Omega_{a_j})(j'\mp\Omega_{a_j}+1)]^{1/2}\delta_{\Omega(\alpha_i),\Omega(\alpha_j)\pm1}\delta_{\Omega(a_i),\Omega(a_j)\mp1}\delta_{K',K}\}. \quad \text{(B11)}$$

In particular for a $K=0$ band with $|\Omega_{\alpha_i}|=|\Omega_{a_i}|=\frac{1}{2}$, one has a diagonal element given by

$$\langle IMK\alpha_ia_i|H_{\rm PP}|IMK\alpha_ia_i\rangle = (-1)^{I+1}\frac{\hbar^2}{2\Im}b_{\alpha_i}b_{a_i}\delta_{K,0}\delta_{|\Omega_{\alpha_i}|,1/2}, \quad \text{(B12)}$$

where

$$b_{\alpha_i}=\sum_j(-1)^{j-1/2}|c^{\alpha_i}{}_{jl}|^2(j+1/2), \quad \text{(B13)}$$

which is commonly called a decoupling parameter.

The $H_{\rm INT}$ term is the most ambiguous and it is hoped that these investigations will help to clarify it. The numerical work involved in computing matrix elements in a basis of Nilsson states is indeed large and it was necessary to assume a central force. This assumption may not adequately apply to off-diagonal matrix elements because frequently Nilsson states are near their asymptotic limit where the projection of orbital and spin-angular momenta as well as the projection of the total particle angular momentum are good quantum numbers. A central force cannot cause scattering between two such asymptotic states unless the projection of orbital angular momentum and spin-angular momentum are the same in both states. The numerical complexity of a tensor force calculation has been postponed until the more realistic diffuse-surface model is used.

Thus the interaction Hamiltonian is written as

$$H_{\rm INT}=U(|\mathbf{r}_{pn}|)[U_1P_M+U_2\boldsymbol{\sigma}_p\cdot\boldsymbol{\sigma}_n+U_3\boldsymbol{\sigma}_p\cdot\boldsymbol{\sigma}_nP_M+U_4]. \quad \text{(B14)}$$

Here $U(|\mathbf{r}_{pn}|)$ is the form of the interaction and in these calculations has a Gaussian shape. The U_i, $i=1,\cdots,4$ are given in terms of the phenomenological two-body force by

$$\begin{aligned}U_1&=\tfrac{1}{8}(V_{\rm SE}-V_{\rm SO}+3V_{\rm TE}-3V_{\rm TO}),\\ U_2&=\tfrac{1}{8}(-V_{\rm SE}-V_{\rm SO}+V_{\rm TE}+V_{\rm TO}),\\ U_3&=\tfrac{1}{8}(-V_{\rm SE}+V_{\rm SO}+V_{\rm TE}-V_{\rm TO}),\\ U_4&=\tfrac{1}{8}(V_{\rm SE}+V_{\rm SO}+3V_{\rm TE}+3V_{\rm TO}).\end{aligned} \quad \text{(B15)}$$

Since $H_{\rm INT}$ does not operate on the collective coordinates, we may write its matrix elements as

$$\langle IMK\alpha_ia_i|H_{\rm INT}|IMK'\alpha_ja_j\rangle = A\delta_{K,K'}+(-1)^IB\delta_{K,K'}\delta_{K,0}, \quad \text{(B16)}$$

where

$$A=(\xi_{\alpha_i}\xi_{a_i},H_{\rm INT}\xi_{\alpha_j}\xi_{a_j}), \quad \text{(B17)}$$

$$B=(-1)^{\pi+1}(\xi_{\alpha_i}\xi_{a_i},H_{\rm INT}\xi_{-\alpha_j}\xi_{-a_j}). \quad \text{(B18)}$$

In general we wish to evaluate matrix elements of the form

$$(\xi_{\alpha_i}\xi_{a_i},H_{\rm INT}\xi_{\alpha_j}\xi_{a_j})=U_1\langle P_M\rangle+U_2\langle\boldsymbol{\sigma}_p\cdot\boldsymbol{\sigma}_n\rangle+U_3\langle\boldsymbol{\sigma}_p\cdot\boldsymbol{\sigma}_nP_M\rangle+U_4\langle1\rangle, \quad \text{(B19)}$$

where we have adopted an obvious notational convenience. After performing some Racah algebra, it is found that

$$\langle P_M\rangle=\sum_{\substack{l_1l_2\\ l_1'l_2'\\ k}} C_1(\alpha_il_1a_il_2\alpha_jl_1'a_jl_2'k), \quad \text{(B20)}$$

$$\langle\boldsymbol{\sigma}_p\cdot\boldsymbol{\sigma}_n\rangle=\sum_{\substack{l_1l_2\\ l_1'l_2'\\ k}} C_2(\alpha_il_1a_il_2\alpha_jl_1'a_jl_2'k), \quad \text{(B21)}$$

$$\langle\boldsymbol{\sigma}_p\cdot\boldsymbol{\sigma}_nP_M\rangle=\sum_{\substack{l_1l_2\\ l_1'l_2'\\ k}} C_3(\alpha_il_1a_il_2\alpha_jl_1'a_jl_2'k), \quad \text{(B22)}$$

$$\langle1\rangle=\sum_{\substack{l_1l_2\\ l_1'l_2'\\ k}} C_4(\alpha_il_1a_il_2\alpha_jl_1'a_jl_2'k), \quad \text{(B23)}$$

where

$$C_1(\alpha_il_1a_il_2\alpha_jl_1'a_jl_2'k) = \frac{(-1)^{\Omega(a_i)+\Omega(a_j)+1}}{(2k+1)^2}\bar{Z}_k[(2l_1+1)(2l_1'+1)(2l_2+1)(2l_2'+1)]^{1/2}$$

$$\times\sum_{uv} a^{\alpha_i}{}_{l_1\Omega(\alpha_i)-u}a^{a_i}{}_{l_2\Omega(a_i)-v}a^{\alpha_i}{}_{l_1'\Omega(\alpha_j)-u}a^{a_i}{}_{l_2'\Omega(a_j)-v}(l_1-\Omega_{\alpha_i}+ul_2'\Omega_{a_j}-v|k-\Omega_{\alpha_i}+\Omega_{a_j}+u-v)(l_1ol_2'o|ko)$$

$$\times(l_2-\Omega_{a_i}+vl_1'\Omega_{\alpha_j}-u|k-\Omega_{a_i}+\Omega_{\alpha_j}+v-u)(l_2ol_1'o|ko), \quad \text{(B24)}$$

$$C_2(\alpha_i l_1 a_i l_2 \alpha_j l_1' a_j l_2' k)$$
$$=\frac{2(-1)^{1+\Omega(a_i)+\Omega(\alpha_j)}}{(2k+1)^2} Z_k[2(2l_1+1)(2l_1'+1)(2l_2+1)(2l_2'+1)]^{1/2}$$
$$\times \sum_{uvu'} a^{\alpha_i}{}_{l_1\Omega(\alpha_i)-u} a^{a_i}{}_{l_2\Omega(a_i)-v} a^{\alpha_i}{}_{l_1'\Omega(\alpha_j)+u'} a^{a_j}{}_{l_2'\Omega(a_j)-u-u'-v} (l_1\Omega_{\alpha_i}-ul_1'-\Omega_{\alpha_j}-u'\,|\,k\Omega_{\alpha_i}-\Omega_{\alpha_j}-u-u')(l_1 0 l_1' 0\,|\,k0)$$
$$\times (l_2\Omega_{a_i}-vl_2'-\Omega_{a_j}+u+v+u'\,|\,k\Omega_{a_i}-\Omega_{a_j}+u+u')(l_2 0 l_2' 0\,|\,k0)(\tfrac{1}{2}u\tfrac{1}{2}u'\,|\,1u+u')(\tfrac{1}{2}v\tfrac{1}{2}-u-u'-v\,|\,1-u-u'), \quad \text{(B25)}$$

$$C_3(\alpha_i l_1 a_i l_2 \alpha_j l_1' a_j l_2' k)$$
$$=\frac{2(-1)^{\Omega(\alpha_i)-\Omega(\alpha_j)}}{(2k+1)^2} \bar{Z}_k[(2l_1+1)(2l_1'+1)(2l_2+1)(2l_2'+1)]^{1/2}$$
$$\times \sum_{uvu'} a^{\alpha_i}{}_{l_1\Omega(\alpha_i)-u} a^{a_i}{}_{l_2\Omega(a_i)-v} a^{\alpha_j}{}_{l_1'\Omega(\alpha_j)+u'} a^{a_j}{}_{l_2'\Omega(a_j)-u-v-u'} (-1)^{-u+v}(l_1\Omega_{\alpha_i}-ul_2'u'+u-\Omega_{a_j}+v\,|\,k\Omega_{\alpha_i}-\Omega_{a_j}+u'+v)$$
$$\times (l_1 0 l_2' 0\,|\,k0)(l_2\Omega_{ai}-vl_1'-\Omega_{\alpha_j}-u'\,|\,k\Omega_{ai}-v-\Omega_{\alpha_j}-u')(l_2 0 l_1' 0\,|\,k0)$$
$$\times (\tfrac{1}{2}u\tfrac{1}{2}u'\,|\,1u+u')(\tfrac{1}{2}v\tfrac{1}{2}-v-u-u'\,|\,1-u'-u), \quad \text{(B26)}$$

$$C_4(\alpha_i l_1 a_i l_2 \alpha_j l_1' a_j l_2' k)$$
$$=\frac{(-1)^{\Omega(a_j)+\Omega(\alpha_j)}}{(2k+1)^2} Z_k[(2l_1+1)(2l_1'+1)(2l_2+1)(2l_2'+1)]^{1/2} \sum_{uv} (-1)^{u+v} a^{\alpha_i}{}_{l_1\Omega(\alpha_i)-u} a^{a_i}{}_{l_2\Omega(a_i)-v} a^{\alpha_j}{}_{l_1'\Omega(\alpha_j)-u} a^{a_j}{}_{l_2'\Omega(a_j)-v}$$
$$\times (l_1\Omega_{\alpha_i}-ul_1'-\Omega_{\alpha_j}+u\,|\,k\Omega_{\alpha_i}-\Omega_{\alpha_j})(l_1 0 l_1' 0\,|\,k0)(l_2\Omega_{a_i}-vl_2'-\Omega_{a_j}+v\,|\,k\Omega_{a_i}-\Omega_{a_j})(l_2 0 l_2' 0\,|\,k0), \quad \text{(B27)}$$

$$Z_k=\int\int R_{n_1 l_1}(p) R_{n_2 l_2}(n) V_k(r_p, r_n) R_{n_1 l_1'}(p) R_{n_2 l_2'}(n) r_p^2 dr_p r_n^2 dr_n, \quad \text{(B28)}$$

$$\bar{Z}_k=\int\int R_{n_1 l_1}(p) R_{n_2 l_2}(n) V_k(r_p, r_n) R_{n_1 l_1'}(n) R_{n_2 l_2'}(p) r_p^2 dr_p r_n^2 dr_n, \quad \text{(B29)}$$

and $(l_1 m_1 l_2 m_2\,|\,l_3 m_3)$ are the usual Clebsch-Gordan coefficients. The phase conventions of Condon and Shortley are adhered to throughout.

In the derivation of all of the above formulas it is assumed that the neutron and proton are above the Fermi sea. If they can be below the Fermi sea then for a one-body operator, certain off-diagonal elements will be different from those given above but they can be related to them by

$$(\xi^{gs}{}_{\alpha i}, \mathbf{O}\xi^{h}{}_{\alpha j}) = S_{-\alpha_j}(\xi_{-\alpha_j}, \mathbf{O}\xi_{-\alpha_i}), \quad \text{(B30)}$$
$$(\xi_{\alpha_i}, \mathbf{O}\xi^{h}{}_{\alpha_j}) = 0, \quad \text{(B31)}$$
$$(\xi^{h}{}_{\alpha i}, \mathbf{O}\xi^{h}{}_{\alpha j}) = -S_{\alpha_i} S_{\alpha_j}(\xi_{-\alpha_j}, \mathbf{O}\xi_{-\alpha_i}). \quad \text{(B32)}$$

Here S_{α_i} is unity if Ω_{α_i} is positive and -1 if Ω_{α_i} is negative. The superscript *gs* refers to the valence particle in its lowest energy state and *h* to a hole excitation, i.e., the valence particle occupies a state below the Fermi surface of the ground-state core. Visualizing the neutron-proton interaction as a product of neutron and proton one-body operators, the appropriate conversions for matrix elements of this two-body operator can easily be deduced.

Programs for the entire calculation were written for use on the LRL IBM 7094 computer. In all cases the maximum prolate deformation ($\eta=6$) was used in computing the Nilsson wave functions. In choosing the nuclear size parameter for the radial wave functions, it was assumed that the oscillator level spacing is $41A^{-1/3}$ MeV and hence

$$\hbar\omega=\hbar^2\nu/m=41A^{-1/3}\ \text{MeV}. \quad \text{(B33)}$$

For evaluating the matrix elements of H_{RPC} and H_{PP}, a value of $\hbar^2/2\Im=9$ keV was assumed for all bands. The force parameters used to compute the spectrum in Fig. 9 are $V_{\text{TE}}=-43.00$ MeV, $V_{\text{TO}}=-43.00$ MeV, $V_{\text{SE}}=-17.20$ MeV, $V_{\text{SO}}=27.95$ MeV, range=1.9 F and $\nu=0.179$ F^{-2}.